$BO55934$

REFRACTORY CERAMICS OF INTEREST IN AEROSPACE STRUCTURAL APPLICATIONS - A MATERIALS SELECTION HANDBOOK

TECHNICAL DOCUMENTARY REPORT NO. RTD-TDR-63-4102, SUPPL. 1

MAY 1964

AMPTIAC

> SEE ALSO
> RTD-TDR-63-4102
> Supplement 1, May 1964
> Supplement 2, April 1965

AF Materials Laboratory
Research and Technology Division
Air Force Systems Command
Wright-Patterson Air Force Base, Ohio

Project No. 7381, Task No. 738105

DISTRIBUTION STATEMENT A
Approved for Public Release
Distribution Unlimited

20011217 162

NOTICES

When Government drawings, specifications, or other data are used for any purpose other than in connection with a definitely related Government procurement operation, the United States Government thereby incurs no responsibility nor any obligation whatsoever; and the fact that the Government may have formulated, furnished, or in any way supplied the said drawings, specifications, or other data, is not to be regarded by implication or otherwise as in any manner licensing the holder or any other person or corporation, or conveying any rights or permission to manufacture, use, or sell any patented invention that may in any way be related thereto.

FOREWORD

This supplemental report was prepared by Battelle Memorial Institute for the United States Air Force on Contract No. AF 33(657)-8326. This contract was initiated under Project No. 7381, "Materials Application", Task No. 738105, "Ceramic and Graphite Technical Information". The work was administered under the direction of the Materials Information Branch, Materials Application Division, Research and Technology Division, at Wright-Patterson Air Force Base, Ohio, with Mr. B. R. Emrich serving as project engineer.

This report covers work conducted from April, 1963, to April, 1964.

The authors would appreciate receiving the comments and criticisms of the users of the Handbook and this supplement to it. Correspondence should be addressed to

Mr. W. H. Duckworth
Chief, Ceramics Division
Battelle Memorial Institute
Columbus, Ohio   43201

ABSTRACT

This publication presents additional refractory-ceramic property data to supplement those published in the first edition of the <u>Materials Selection Handbook</u>, issued in October, 1963, as RTD-TDR-63-4102.

The materials covered are nonmetallic inorganic crystalline materials with melting points above 2730 F (1500 C), including intermetallic compounds and excluding glass, carbon, and graphite. The data are from literature published in 1961 and 1962.

This technical documentary report has been reviewed and is approved.

D. A. SHINN
Chief, Materials Information Branch
Materials Applications Division
AF Materials Laboratory

TABLE OF CONTENTS

INTRODUCTION

Primarily because of their heat-resistant qualities ceramics are recognized as an important class of materials for aerospace application. To facilitate designing of aerospace systems, the compilation of reliable property data on refractory ceramics (nonmetallic inorganic crystalline materials, including intermetallic materials) has been a continuing effort of the Air Force. The most recent compilation was RTD-TDR-63-4102, "Refractory Ceramics of Interest in Aerospace Structural Applications — A Materials Selection Handbook", dated October 1963.* Data contained in the Handbook were obtained from the literature to 1962. Updating and upgrading of this Handbook has been a subsequent activity at Battelle under Air Force Contract AF 33(657)-8326. In this project, additional property data on pertinent materials were obtained from the open literature through 1962, and are presented in this supplement to the Handbook.

Like the Handbook, the supplement includes the compilation of selected property data on refractory nonmetallic inorganic crystalline materials, including intermetallic compounds. Only materials having melting points above 2730 F (1500 C) were included. Glass, carbon, and graphite are excluded. Also, data were limited to materials in which the principal crystalline phase exceeds 95 per cent by weight. The data of interest included but were not limited to mechanical properties (strength, elastic modulus, Poisson's ratio, creep, etc.); thermal properties (expansion, conductivity, specific heat, etc.); and certain physical properties (crystal structure, density, melting point, etc.).

The format of this supplement is generally the same as that of the Handbook.

The section "Materials Index and Property Indicator", beginning on page 3, provides an alphabetical listing of all materials included in the supplement. In addition to giving the page where the detailed information on each material begins, it also indicates by an "x" those properties for which new or complementary information was found in the literature.

As in the Handbook, the section "Detailed Properties of Materials", which begins on page 7, is divided into 10 subsections according to material class; the materials are grouped, in general, according to the group of the cation in the Periodic Table. Properties are presented in the order of (1) physical, (2) thermal, (3) mechanical, and (4) other properties. Test-specimen characterization and test conditions are tabulated as reference information, when possible. A list of the literature referred to follows the presentation of properties.

Appendix A contains a dissertation on available analytical techniques for describing strength characteristics of brittle materials.

ALUMINUM NIOBATE – NEODYMUM-TELLURIUM

Material	Chemical Formula	Page	Density	Melting Point	Specific Heat	Thermal Conductivity	Thermal Expansion	Elastic Modulus	Modulus of Rigidity	Poisson's Ratio	Bend Strength	Tensile Strength	Compressive Strength	Impact Strength	Hardness	Creep	Thermal Shock	Oxidation Corrosion
Aluminum Niobate	$Al_2O_3 \cdot Nb_2O_5$	40	x	x														
Aluminum Oxide	Al_2O_3	29	x			x	x	x			x							
Barium Boride	BaB_6	9					x											
Beryllium Oxide	BeO	32				x	x				x							
Boron Silicide	B_4Si	49	x			x	x	x			x				x			x
	B_6Si	49	x			x	x	x			x				x			x
Calcium Boride	CaB_6	9					x											
Calcium Niobate	$CaO \cdot Nb_2O_5$	40	x	x														
	$2CaO \cdot Nb_2O_5$	40	x	x														
	$3CaO \cdot Nb_2O_5$	40	x	x														
Cerium Boride	CeB_6	12					x											
Cerium-Selenium	$CeSe$	52		x														
	Ce_2Se_3	52		x														
Cerium-Tellurium	$CeTe$	52		x														
	Ce_2Te_3	52		x														
Chromium Carbide	$Cr_{23}C_6$	17				x												
	Cr_7C_3	17				x												
	Cr_3C_2	17				x												
Chromium Silicide	Cr_3Si	45					x											
	Cr_5Si_3	45					x											
	$CrSi$	45					x											
Dysprosium Boride	DyB_6	12																x
Europium Boride	EuB_6	12					x											x
Europium Oxide	Eu_2O_3	36	x															x
Erbium-Selenium	Er_2Se	52		x														
Gadolinium Boride	GdB_6	12					x											
Gadolinium-Selenium	$GdSe$	52		x														
Gadolinium-Tellurium	$GdTe$	52		x														
Hafnium Carbide	HfC	15			x													
Hafnium Nitride	HfN	25				x												
Hafnium Titanate	$HfO_2 \cdot TiO_2$	40	x	x														
Lanthanum Boride	LaB_6	12					x											
Lanthanum Silicide	$LaSi_2$	47					x											
Magnesium Germanate	$MgO \cdot GeO_2$	40	x	x														
	$2MgO \cdot GeO_2$	40	x	x														
	$4MgO \cdot GeO_2$	40	x	x														
Magnesium Oxide	MgO	34						x										
Molybdenum Carbide	MoC	17		x														
Molybdenum Silicide	Mo_3Si	45					x											
	Mo_5Si_3	45					x											
	$MoSi_2$	45					x						x		x			
Neodymium Boride	NdB_6	12					x											
Neodymium-Tellurium	$NdTe$	52		x														
	Nd_3Te_4	52		x														

NIOBIUM BORIDE – THORIUM SULFIDE

Material	Chemical Formula	Page	Density	Melting Point	Specific Heat	Thermal Conductivity	Thermal Expansion	Elastic Modulus	Modulus of Rigidity	Poisson's Ratio	Bend Strength	Tensile Strength	Compressive Strength	Impact Strength	Hardness	Creep	Thermal Shock	Oxidation Corrosion
Niobium Boride	Nb_3B_2	11		x											x			
	Nb_2B	11		x											x			
	NbB	11		x											x			
	Nb_3B_4	11		x											x			
	NbB_2	11		x											x			
Niobium Nitride	Nb_2N	26				x												
	NbN	26				x												
Niobium-Phosphorous	Nb-P	52	x	x											x			x
Niobium Silicide	$NbSi_2$	44					x											
Niobium-Tellurium	NbTe	52		x														
Plutonium Carbide	PuC	20					x											
	Pu_2C_3	20					x											
Praeseodymium Silicate	$Pr_2O_3 \cdot SiO_2$	39	x	x														
	$2Pr_2O_3 \cdot 3SiO_2$	39	x	x														
	$Pr_2O_3 \cdot 2SiO_2$	39	x	x														
Rhenium Silicide	$ReSi_2$	49					x											
Samarium Boride	SmB_6	12																x
Samarium Oxide	Sm_2O_3	37																x
Samarium-Selenium	SmSe	52		x														
Samarium-Tellurium	SmTe	52		x														
Scandium Carbide	ScC	18	x	x			x								x			
Scandium Silicate	$Sc_2O_3 \cdot SiO_2$	39	x	x														
	$Sc_2O_3 \cdot 2SiO_2$	39	x	x														
Silicon Carbide	SiC	14											x					
Silicon Nitride (α, β)	Si_3N_4	23	x								x				x	x		x
Strontium Boride	SrB_6	9					x											
Tantalum Boride	Ta_2B	11		x														
	Ta_3B_2	11		x											x			
	TaB	11		x											x			
	Ta_3B_4	11		x											x			
	TaB_2	11		x											x			
Tantalum Carbide	TaC	16											x					
Tantalum Nitride	Ta_2N	26				x												
	TaN	26				x												
Tantalum-Phosphorous	TaP	52	x	x											x			x
Tantalum Silicide	$TaSi_2$	44					x											
Thorium Aluminide	Th_2Al	42	x												x			x
Thorium Beryllide	$ThBe_{13}$	42	x												x			x
Thorium Boride	ThB_4	13													x			x
Thorium Carbide	ThC	20				x									x			x
	ThC_2	20				x	x								x			x
Thorium Oxide	ThO_2	38					x											
Thorium Silicide	Th_3Si_2	48	x												x			x
	ThSi	48	x												x			x
Thorium Sulfide	ThS	41					x				x				x			

Material	Chemical Formula	Page	Density	Melting Point	Specific Heat	Thermal Conductivity	Thermal Expansion	Elastic Modulus	Modulus of Rigidity	Poisson's Ratio	Bend Strength	Tensile Strength	Compressive Strength	Impact Strength	Hardness	Creep	Thermal Shock	Oxidation Corrosion
Titanium Boride	TiB_2	10				x												
Titanium Carbide	TiC	15			x	x												
Titanium Nitride	TiN	25				x									x			
Titanium-Phosphorus	TiP	52	x	x											x			x
Titanium Silicide	Ti_5Si_3	43					x											
	$TiSi$	43					x											
	$TiSi_2$	43					x											
Tungsten Carbide	WC	17		x														
Tungsten Silicide	WSi_2	45					x											
Uranium Carbide	UC	20				x									x			x
Uranium Nitride	UN	27				x	x				x				x			
Uranium Oxide	UO_2	38				x												
Uranium Sulfide	US	41					x				x				x			
Vanadium Carbide	VC	16				x												
Vanadium Nitride	VN	26				x												
Vanadium Silicide	V_3Si	44					x											
	V_5Si_3	44					x											
	VSi_2	44					x											
Ytterbium-Tellurium	$YbTe$	52		x														
Yttrium Boride	YB_6	12																x
Yttrium Carbide	YC	18	x	x			x								x			x
	Y_2C_3	18	x	x											x			x
	YC_2	18	x	x											x			x
Yttrium Oxide	Y_2O_3	36				x												
Yttrium Silicate	$Y_2O_3 \cdot SiO_2$	39	x	x														
	$2Y_2O_3 \cdot 3SiO_2$	39	x	x														
	$Y_2O_3 \cdot 2SiO_2$	39	x	x														
Yttrium-Tellurium	Y_2Te_3	52		x														
Zirconium Boride	ZrB_2	10									x							
Zirconium Carbide	ZrC	15			x	x												
Zirconium Nitride	ZrN	25				x									x			
Zirconium Oxide	ZrO_2	35				x	x											

DETAILED PROPERTIES OF MATERIALS

CONTENTS

BORIDES OF BARIUM, BERYLLIUM, CALCIUM, MAGNESIUM, AND STRONTIUM (ALKALINE-EARTH METALS)
[See pages 51 and 52 of Handbook]

THERMAL PROPERTIES

TABLE 1. AVERAGE COEFFICIENTS OF LINEAR THERMAL EXPANSION OF HEXABORIDES OF BARIUM, CALCIUM, AND STRONTIUM[617]

Boride	Temperature Range, F	Thermal Expansion Coefficients[a], $10^{-6}/F$
BaB_6	68-1472	3.7
CaB_6	68-1472	3.6
SrB_6	68-1472	3.7

(a) Calculated from X-ray lattice parameters of powder samples prepared by reducing oxides of the metals with boron.

MECHANICAL PROPERTIES

Microhardness of strontium hexaboride (SrB_6) is reported as 2900 ± 90 kg/mm^2 for a 20-g load. Specimens were hot pressed and had a residual porosity of about 10 per cent.[603]

OTHER PROPERTIES

Oxidation and Corrosion Resistance

Powders of alkaline-earth hexaborides Ba, Ca, and Sr have poor oxidation resistance above 1100 F. Nitrogen at high temperatures does not decompose these borides or form nitrides. No reaction with carbon up to 3600 F is indicated. These borides also are resistant to the action of acids (except nitric) and alkalis.[614]

BORIDES OF TITANIUM, ZIRCONIUM, AND HAFNIUM

[See pages 53-63 of Handbook]

THERMAL PROPERTIES

Titanium Diboride (TiB$_2$):

    Thermal conductivity, room temperature - 34.8 Btu/(hr)(ft)(F). Determined by static method; value calculated for zero porosity.[584]

MECHANICAL PROPERTIES
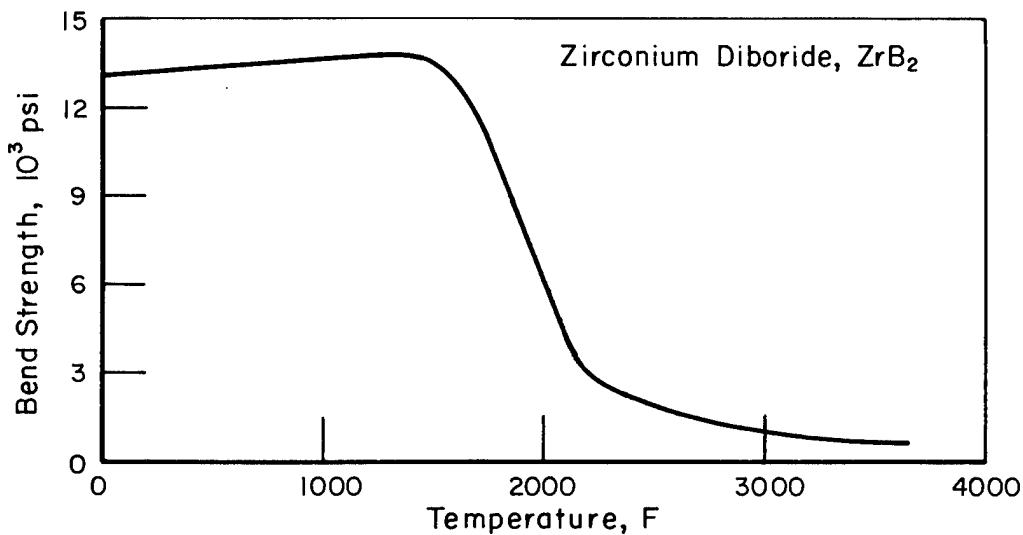
FIGURE 1. BEND STRENGTH OF HIGH-POROSITY ZIRCONIUM DIBORIDE[580]

    Specimens with 20 to 25 per cent porosity were resistively heated in argon atmosphere and loaded at a rate of 550 psi per second using center-point loading.

BORIDES OF VANADIUM, NIOBIUM, AND TANTALUM

[See pages 65-70 of Handbook]

PHYSICAL AND MECHANICAL PROPERTIES

TABLE 2. PHYSICAL AND MECHANICAL PROPERTIES OF NIOBIUM AND TANTALUM BORIDES[593]

Boride	Formula	Crystal Structure	Melting Point, F	Microhardness[a], kg/mm^2
Niobium	Nb$_3$B$_2$	Tetragonal	2912[c]	1720
	Nb$_2$B	Tetragonal	2912[c]	2060
	NbB	Orthorhombic	4136[d]	2200
	Nb$_3$B$_4$	Orthorhombic	4892[c]	2290
	NbB$_2$	Hexagonal	5432[d]	2600[b]
Tantalum	Ta$_2$B	Tetragonal	3488[c]	--
	Ta$_3$B$_2$	Tetragonal	3668[c]	2770
	TaB	Orthorhombic	4406[d]	3120
	Ta$_3$B$_4$	Orthorhombic	4802[c]	3350
	TaB$_2$	Hexagonal	5644[d]	--

(a) 50-gram load.
(b) 30-gram load.
(c) Incongruent melting point.
(d) Congruent melting point.

BORIDES OF THE RARE-EARTH METALS

[See pages 79-82 of Handbook]

THERMAL PROPERTIES

TABLE 3. AVERAGE COEFFICIENTS OF LINEAR THERMAL EXPANSION OF VARIOUS HEXABORIDES OF RARE-EARTH METALS[617]

Boride	Thermal Expansion Coefficient[a], $10^{-6}/F$	Boride	Thermal Expansion Coefficient[a], $10^{-6}/F$
CeB_6	4.0	PrB_6	4.2
EuB_6	3.8	SmB_6	3.8
GdB_6	4.8	TbB_6	4.3
LaB_6	3.6	YB_6	3.6
NdB_6	4.0	YbB_6	3.2

(a) Values calculated from X-ray lattice parameters determined on powder samples for temperature range of 68-1472 F.

OTHER PROPERTIES

Oxidation Resistance

Hot-pressed specimens of DyB_6, EuB_6, YB_6, and SmB_6 all lost considerable weight, but exhibited no dimensional change, in a steam environment (750 F, 1500 psi, and 500 hours). Yttrium tetraboride (YB_4) was essentially unchanged after 500 hours of exposure at 1500 psi and 400 F to 1000 F. General conclusion by Hoyt[574] was that rare-earth borides are much less resistant to oxidation than are transition-metal borides.

BORIDES OF THORIUM AND URANIUM

[See pages 83-87 of Handbook]

MECHANICAL PROPERTIES

The microhardness (Knoop) of thorium tetraboride (ThB_4) is reported as 2043 for a 100-g load at room temperature.[568]

OTHER PROPERTIES

Oxidation Resistance

A weight gain of 0.22 mg/cm^2/hr was measured after exposure of ThB_4 at 1100 F in dry air flowing. A similar ThB_4 specimen exposed to dry CO_2 at similar flow rate had a weight gain of 0.08 mg/cm^2/hr. Specimens were arc melted and of high purity.[568]

SILICON CARBIDE (SELF-BONDED)

[See pages 105-112 of Handbook]

MECHANICAL PROPERTIES

Silicon Carbide (Whiskers):

 Tensile strength — 100,000 to 1,650,000 psi

 Elastic deformation — Up to 1.1 per cent

The whiskers were prepared by pyrolysis and reaction of methyltrichlorsilane in hydrogen; hexagonal crystal form; density of 3.214 to 3.217 g/cm^3.[616]

 Unpublished data by other investigators indicates tensile strengths over 2×10^6 psi for silicon carbide filaments.

CARBIDES OF TITANIUM, ZIRCONIUM, AND HAFNIUM

[See pages 113-126 of Handbook]

PHYSICAL PROPERTIES

Melting points of specimens of TiC, ZrC, and HfC were 5324, 6440, and 7034 F, respectively. [567] Pressed and sintered specimens were heated in an arc furnace; temperature was measured at liquid-solid boundary.

THERMAL PROPERTIES
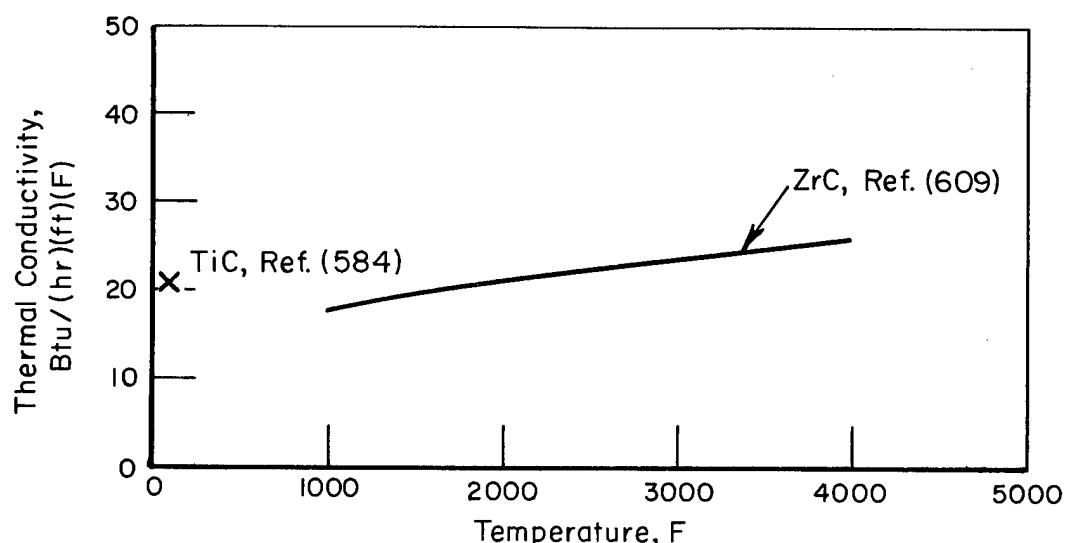
FIGURE 2. THERMAL CONDUCTIVITY OF TITANIUM AND ZIRCONIUM CARBIDES

Reference	Reference Information
(584)	Static method; value calculated for zero porosity
(609)	Steady-state, radial-heat-flow method; hot-pressed specimen; 95 per cent theoretical density; 50-micron average grain size.

CARBIDES OF VANADIUM, NIOBIUM, AND TANTALUM

[See pages 127-134 of Handbook]

PHYSICAL PROPERTIES

Melting points of specimens of VC, NbC, and TaC were 5036, 6188, and 6206 F, respectively.[567] Pressed and sintered specimens were heated in our arc furnace; temperature was measured at liquid-solid boundary.

THERMAL PROPERTIES

Vanadium Carbide (VC):

Thermal conductivity — 14.3 Btu/(hr) (ft) (F) at 72 F.[584] Determined by static method; value calculated for zero porosity.

MECHANICAL PROPERTIES

Tantalum Carbide (TaC):

Tensile strength — $30\text{-}35 \times 10^3$ psi at 72 F.[565] Six filamentary specimens, 0.005-0.015-in. diameter, prepared by gas-phase carburization of tantalum wire.

CARBIDES OF CHROMIUM, MOLYBDENUM, AND TUNGSTEN

[See pages 135-144 of Handbook]

PHYSICAL PROPERTIES

Melting points of specimens of MoC and of WC were 5198 and 5108 F, respectively.[567] Pressed and sintered specimens were heated in an arc furnace; temperatures were measured at liquid-solid boundary.

THERMAL PROPERTIES

TABLE 4. THERMAL CONDUCTIVITY OF CHROMIUM
CARBIDES AT 70 F[584]

Carbide	Thermal Conductivity[a], Btu/(hr) (ft) (F)
$Cr_{23}C_6$	10.6
Cr_7C_3	8.7
Cr_3C_2	11.1

(a) Static method; value calculated for zero porosity.

CARBIDES OF THE RARE-EARTH METALS

[See pages 145-146 of Handbook]

Data on scandium and yttrium carbides were given in References (601) and (602). All properties are for hot-pressed specimens.

PHYSICAL PROPERTIES

TABLE 5. PHYSICAL PROPERTIES OF SCANDIUM AND YTTRIUM CARBIDES

Carbide	Pycnometer Density, g/cm^3	Melting Point, F	Reference
ScC	3.06	--	(602)
YC	3.50	3540	(601)
Y_2C_3	3.66	3270	(601)
YC_2	3.95	4170	(601)

THERMAL PROPERTIES

TABLE 6. COEFFICIENT OF LINEAR THERMAL EXPANSION FOR SCANDIUM CARBIDE

Carbide	Temperature Range, F	Thermal Expansion Coefficient, $10^{-6}/F$	Reference
ScC	None given	6.3	(602)

MECHANICAL PROPERTIES

TABLE 7.   MICROHARDNESS OF SCANDIUM AND
                    YTTRIUM CARBIDES

Carbide	Microhardness, kg/mm^2	Load, g	Reference
ScC	2700	Not given	(602)
YC	120 ± 33	5	(601)
Y_2C_3	900 ± 160	50	(601)
YC_2	700 ± 106	50	(601)

OTHER PROPERTIES

Oxidation and Corrosion Resistance
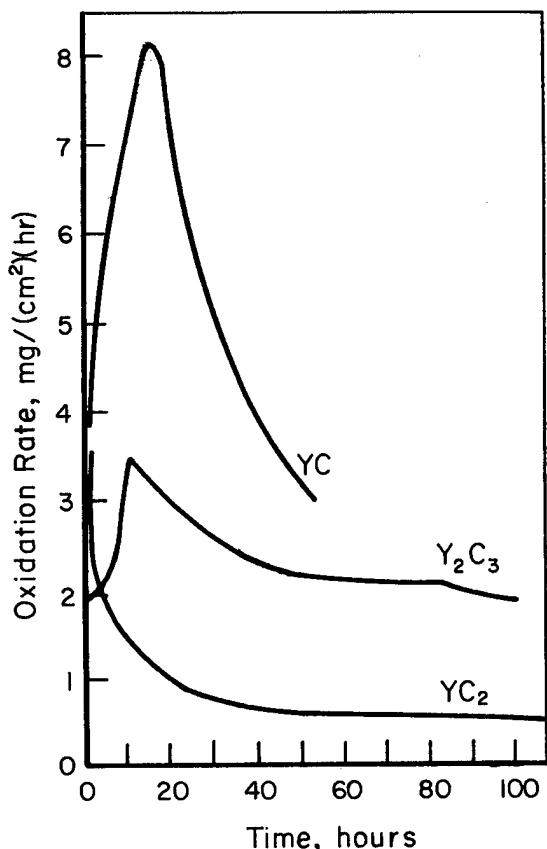
FIGURE 3.   OXIDATION RATE OF
    YTTRIUM CARBIDES IN STATIC
    AIR AT ROOM TEMPERATURE[601]

    Powders of the yttrium carbides are readily decomposed by water, dilute acids, and alkalies; reaction rates are low in concentrated acids. YC has the greatest chemical resistance.[601]

CARBIDES OF THORIUM, URANIUM, AND PLUTONIUM

[See pages 147-151 of Handbook]

THERMAL PROPERTIES

TABLE 8. THERMAL CONDUCTIVITY OF THORIUM AND
URANIUM CARBIDES

Carbide	Temperature, F	Thermal Conductivity, Btu/(hr) (ft) (F)	Reference[a]
ThC	75	16.7	(579)
ThC_2	75	13.8	(579)
$UC_{0.94}$	480	14.7	(562)
UC	480	13.3	(562)
$UC_{1.06}$	480	13.8	(562)

(a) Reference	Reference Information
(579)	Arc-melted and cast rod specimens; values calculated from Wiedemann-Franz relationship.
(562)	Arc-melted and cast ingots; 99 per cent dense; axial-heat-flow method.

TABLE 9. AVERAGE COEFFICIENTS OF LINEAR THERMAL EXPANSION
OF THORIUM AND PLUTONIUM CARBIDES

Carbide	Temperature Range, F	Thermal Expansion Coefficient, $10^{-6}/F$	Reference[a]
ThC_2	32-1800	4.7	(588)
PuC	68-1435	5.95	(594, 582)
Pu_2C_3	68-1435	8.2	(594)

(a) Reference	Reference Information
(594)	Calculated from X-ray lattice constants of powder samples indicated to be of high purity.
(588)	Dilatometer method; no data on material were given.
(582)	Dilatometer method; specimens arc melted and cast; 95 per cent dense; 95 per cent purity.

MECHANICAL PROPERTIES

TABLE 10. MICROHARDNESS OF THORIUM CARBIDES

Carbide	Microhardness, kg/mm^2	Load, g	Reference[a]
ThC	850	200	(579)
ThC$_2$	600	200	(579)

(a) Reference   Reference Information
       (579)   Arc-melted and cast rod specimens; values calculated from
                    Wiedemann-Franz relationship.
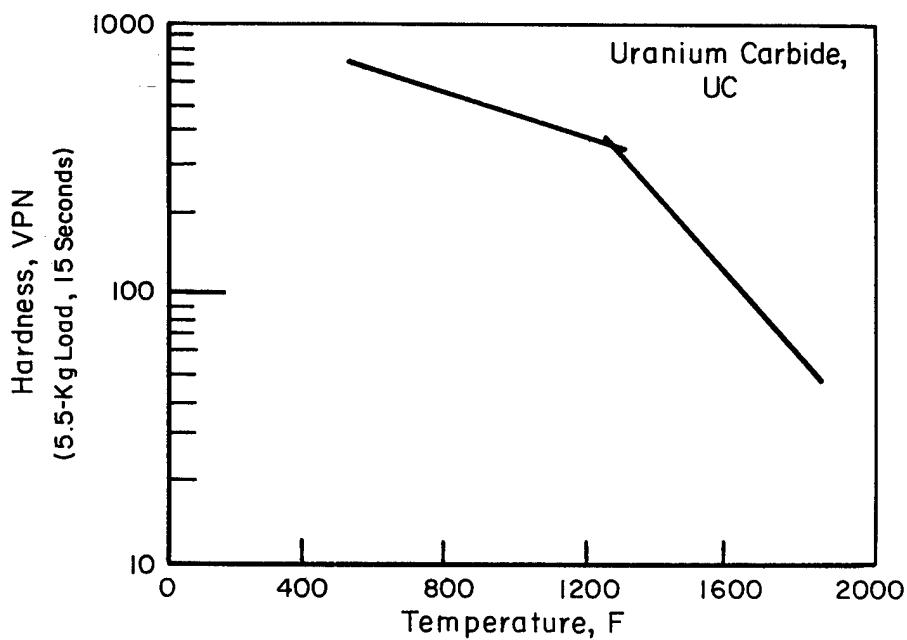
FIGURE 4. TYPICAL MICROHARDNESS OF URANIUM CARBIDE
             AT ELEVATED TEMPERATURES[562]

          Arc-melted and cast specimens, 99 per cent dense.

OTHER PROPERTIES

Oxidation and Corrosion Resistance
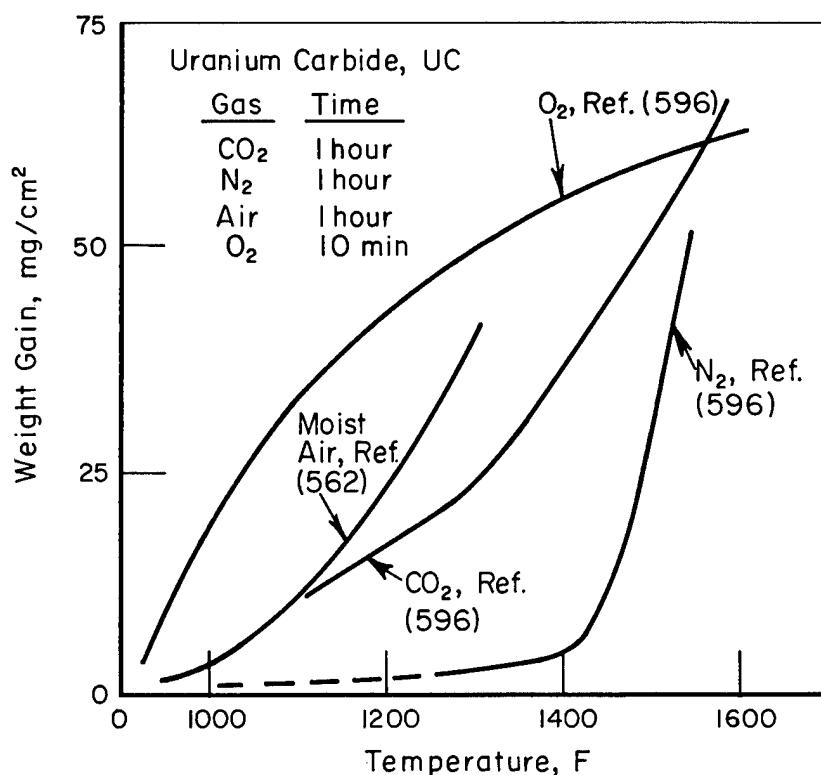
FIGURE 5. WEIGHT CHANGE OF URANIUM CARBIDE IN VARIOUS
GASEOUS ENVIRONMENTS

Reference	Reference Information
(596)	Disk specimens, 0.6-inch diameter, 0.2-inch thick (11.7-12.7 g/cm^3 density); exposure in CO_2, O_2, or N_2 at 1-atmosphere pressure and 500 cm^3/min flow rate
(562)	Arc-melted and cast ingots, 99 per cent dense; static air containing 1 per cent of water.

A weight gain of 0.95 and 4.2 $mg/cm^2/hr$ was measured for ThC and ThC_2, respectively, after exposure at 1100 F in dry flowing air.[568] Specimens were arc melted and of high purity.

SILICON NITRIDE

[See pages 169-176 of Handbook]

PHYSICAL PROPERTIES

TABLE 11. THEORETICAL DENSITIES OF Si_3N_4 PHASES

Phases	Theoretical Density[a], g/cm^3	References
α Si_3N_4	3.184	(597)
β Si_3N_4	3.187	(597)

(a) Calculated from X-ray lattice constants.

   α Si_3N_4:   a = 7.748 and c = 5.617

   β Si_3N_4:   a = 7.608 and c = 2.911.

MECHANICAL PROPERTIES
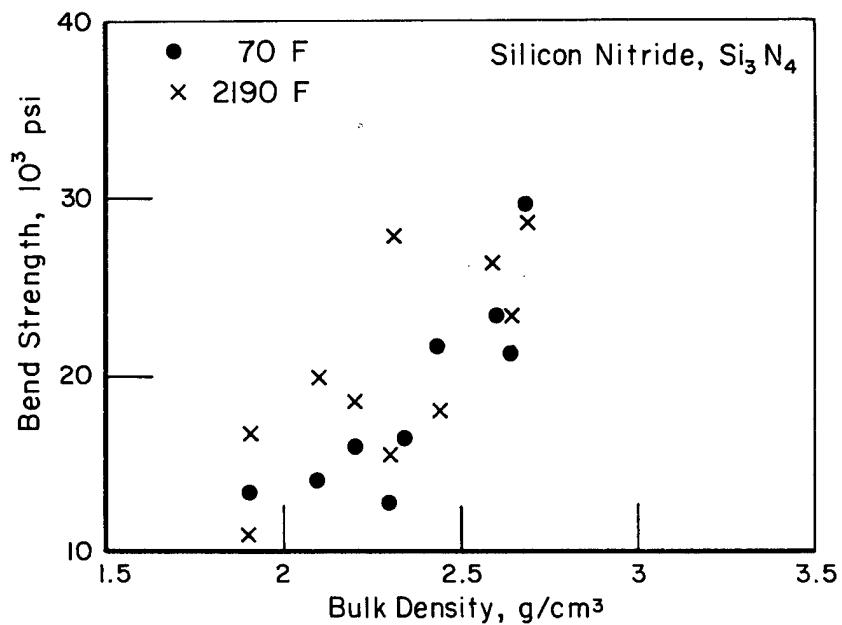
FIGURE 6. BEND STRENGTH OF SILICON NITRIDE[595]

Specimens were reaction sintered, with
phases as follows: 0-95% α Si_3N_4; 5-100%
β Si_3N_4; 0-3% silicon metal.

MECHANICAL PROPERTIES (Continued)

TABLE 12. BEND STRENGTH, CREEP RATE, AND HARDNESS OF
SILICON NITRIDE WITH MgO ADDITIONS[564]

MgO, weight per cent	Apparent Porosity, per cent	Bend Strength, 10^3 psi	Relative Creep Rate [a]	Microhardness, (VPN) kg/mm^2
1.3	2.8	50	1.0	810
3.3	0.5	68	3.4	1500
5.0	0.08	77	4.2	1620
6.7	0.22	65	0.8	1670
8.4	0.17	68	0.3	1660
10.0	0.07	40	0.5	1670

Laboratory-prepared silicon nitride powder was milled with MgO and the mixtures hot pressed at 3360 F and 3000 psi; no specimen size was given.

(a) 2190 F, 8000 psi.

TABLE 13. PROPERTIES OF SILICON NITRIDE (PRESSURE SINTERED)
WITH 5 PER CENT MAGNESIA[564]

Bulk Density, g/cm^3	3.12-3.18
Linear Thermal Expansion Coefficient, 10^{-6}/F	1.5
Bend Strength, 10^3 psi	
At 70 F	80-100
At 2190 F	50-70
Young's Modulus, 10^6 psi	31.5
Microhardness (VPN), kg/mm^2	1600-1800
Crystalline Form, per cent:	
α silicon nitride	0-30
β silicon nitride	70-100
Oxidation Resistance	1 mg/cm^2 gain in 100 hr at 2000 F

The microhardness (DPH) of reaction-sintered specimens of α silicon nitride was reported to be 300 kg/mm^2 (50-g load) and of β silicon nitride 2300 kg/mm^2 (50-g load).[598]

NITRIDES OF TITANIUM, ZIRCONIUM, AND HAFNIUM

[See pages 177-184 of Handbook]

THERMAL PROPERTIES

Thermal conductivities of TiN, ZrN, and HfN at room temperature are reported to be 10.9, 11.6, and 12.5 Btu/(hr) (ft) (F), respectively[584]. The static method was used; values were calculated to zero porosity.

MECHANICAL PROPERTIES

TABLE 14. MICROHARDNESS OF TITANIUM AND
ZIRCONIUM NITRIDES[604]

Nitride Phase	Microhardness[a], kg/mm^2
$TiN_{0.59}$	1200 ± 137
$TiN_{0.63}$	1400 ± 182
$TiN_{0.85}$	1630 ± 101
$TiN_{0.92}$	1780 ± 51
$TiN_{0.97}$	1900 ± 182
$ZrN_{0.91}$	1480 ± 85

(a) Reaction-sintered specimens; 50-g load; room temperature.

NITRIDES OF VANADIUM, NIOBIUM, AND TANTALUM

[See pages 185-188 of Handbook]

THERMAL PROPERTIES

TABLE 15. THERMAL CONDUCTIVITY OF VANADIUM,
NIOBIUM, AND TANTALUM NITRIDES[584]

Nitrides	Thermal Conductivity at Room Temperature[a], Btu/(hr)(ft)(F)
VN	6.5
Nb$_2$N	4.8
NbN	2.1
Ta$_2$N	5.8
TaN	4.8

(a) Static method; values calculated to zero porosity.

NITRIDES OF THORIUM, URANIUM, AND PLUTONIUM

[See pages 193-194 of Handbook]

THERMAL PROPERTIES

TABLE 16. COEFFICIENT OF LINEAR THERMAL EXPANSION
OF URANIUM MONONITRIDE (UN)

Temperature Range, F	Average Thermal Expansion Coefficient, 10^{-6}/F	Reference[a]
425-2190	~5.4	(610)
212-2900	~5.5	(578)

(a)	Reference	Reference Information
	(610)	79-84 per cent dense specimens
	(578)	95 per cent dense specimens.
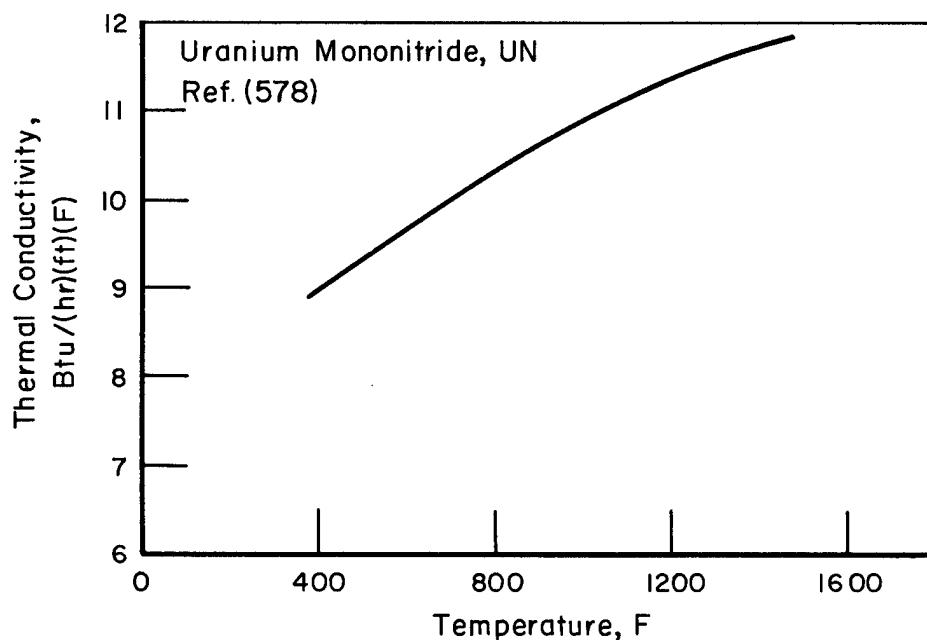
FIGURE 7. THERMAL CONDUCTIVITY OF URANIUM MONONITRIDE[578]

Specimens were 95 per cent dense.

MECHANICAL PROPERTIES

TABLE 17. MECHANICAL PROPERTIES OF URANIUM MONONITRIDE (UN)

Property	Temperature, F	Property Value	Reference[a]
Bend Strength, 10^3 psi	77	10.5	(610)
	1472	11.2	
	2192	19.3	
	2552	13.7	
	2912	Deformed	
Young's Modulus, 10^6 psi			
Static	77	21.6	(610)
Dynamic	77	31	
Shear Modulus, 10^6 psi	77	8.7	(610)
Poisson's Ratio	77	0.24	(610)
Hardness, kg/mm^2	77	600 Knoop	(578)

(a)   Reference   Reference Information

   (610)   79-84 per cent dense specimens

   (578)   95 per cent dense specimens.

ALUMINUM OXIDE

[See pages 205-218 of Handbook]

THERMAL PROPERTIES

Thermal Expansion

    Wachtman et al. [618] provides a reference to complement the data in the Handbook on linear thermal expansion of single crystal and polycrystalline alumina (Al_2O_3). Measurements were made with interferometric apparatus; also, calculations were made by using Grüneisen's equation. Specimens included Linde synthetic sapphire and a polycrystalline Al_2O_3 (3. 97 g/cm^3).

Thermal Conductivity
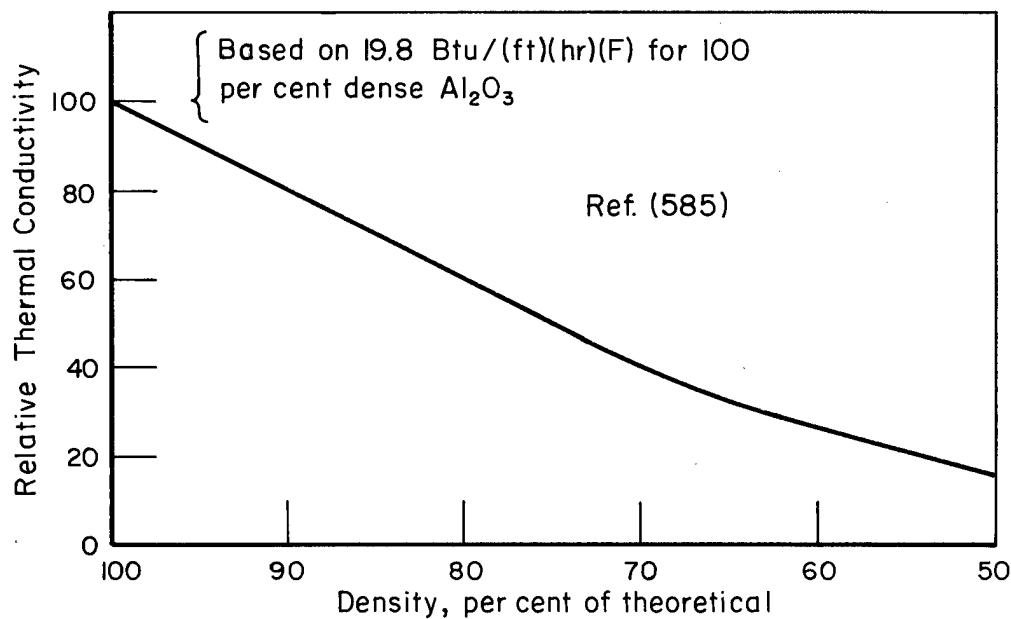
FIGURE 8.   EFFECT OF DENSITY ON THERMAL CONDUCTIVITY
            OF ALUMINA[585]

            Hot-pressed alumina. Density range obtained by
            variation in forming temperature and pressure.
            Axial-heat-flow method used in measurements of
            heat conductivity.

MECHANICAL PROPERTIES
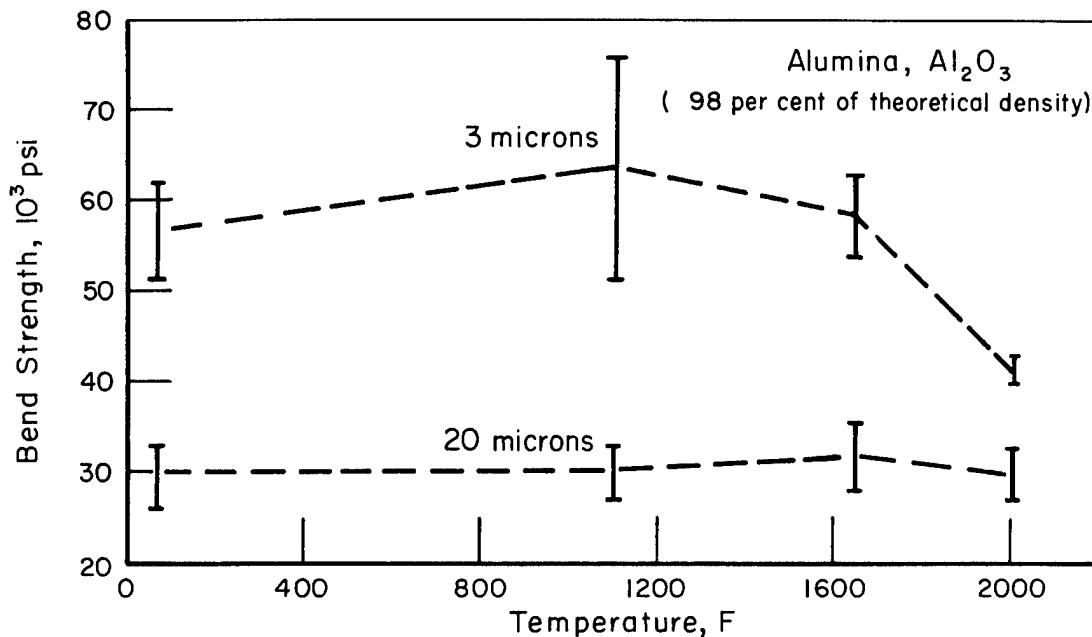
Bend Strength

FIGURE 9. EFFECT OF GRAIN SIZE AND TEMPERATURE ON
BEND STRENGTH OF ALUMINA[563]

See page 31 for reference information.

Modulus of Elasticity
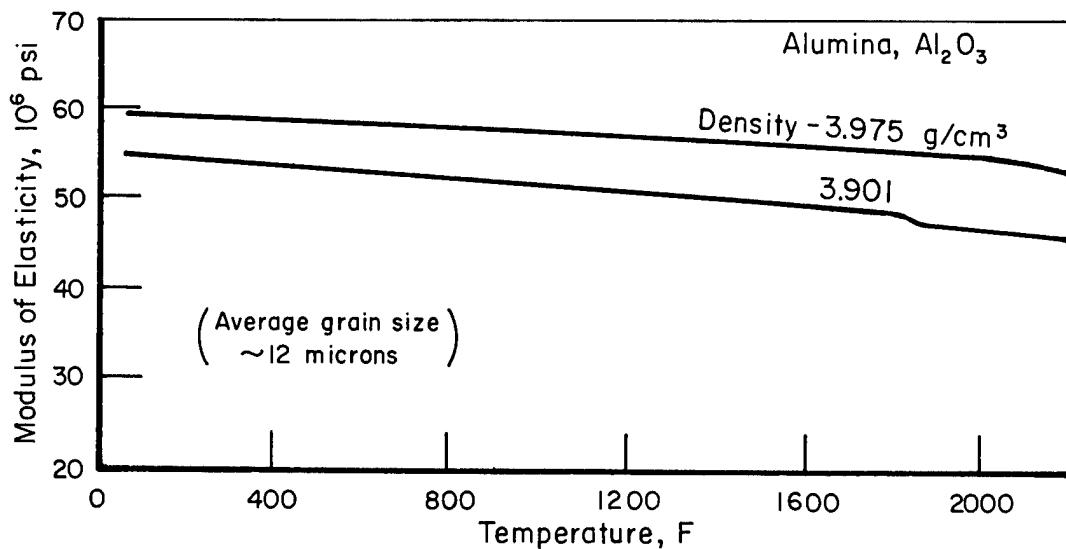
FIGURE 10. YOUNG'S MODULUS FOR HIGH-DENSITY, FINE-GRAIN ALUMINA[563]

See page 31 for reference information.

MECHANICAL PROPERTIES

Modulus of Elasticity (Continued)
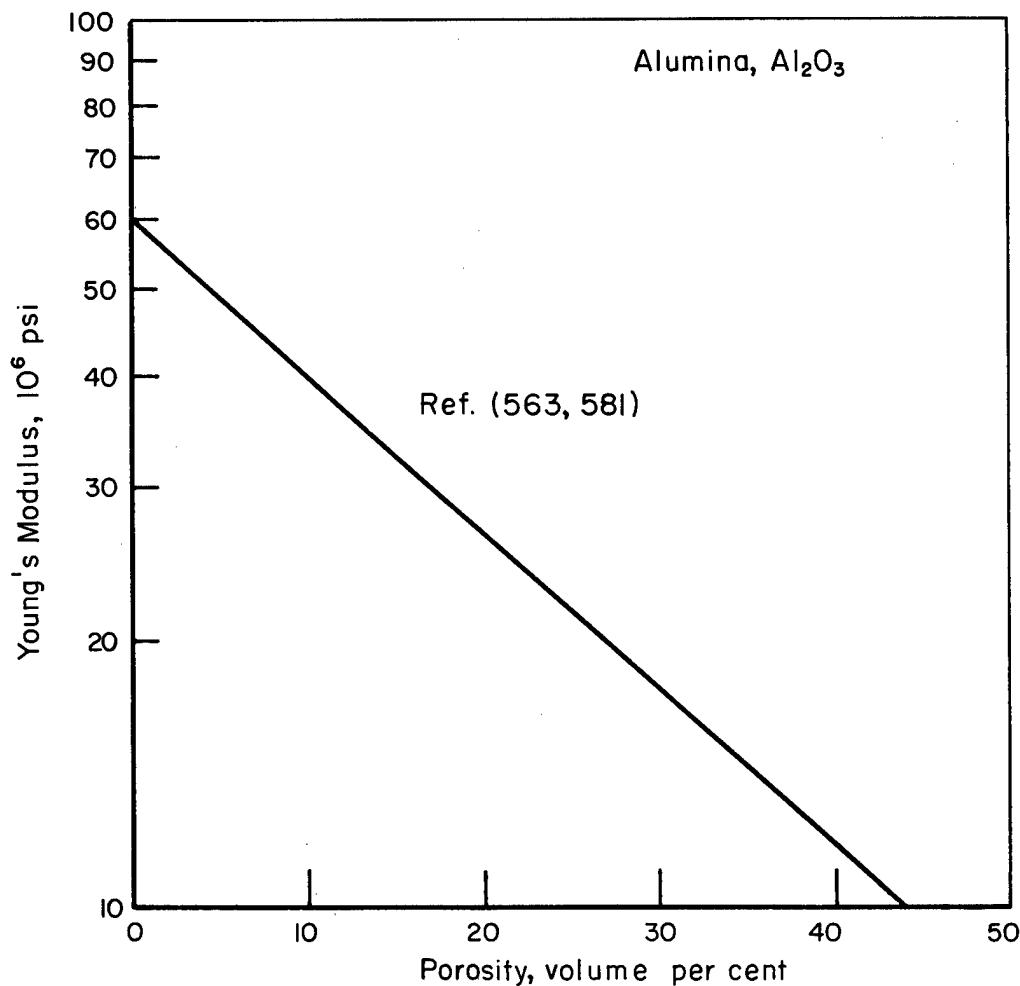
FIGURE 11. EFFECT OF POROSITY ON MODULUS OF ELASTICITY
OF ALUMINA[563,581]

Reference Information for Figures 9, 10, and 11

Reference	Material and Testing Details
(563)	Hot-pressed specimens, prepared from alumina powder of 99.5 per cent purity, had less than 2 per cent total porosity. Bend strength determined using center-point loading; the span was 0.8 inch and the depth-to-span ratio was 0.19. Dynamic method used for Young's modulus.
(581)	Young's modulus data from various investigators.

BERYLLIUM OXIDE

[See pages 219-226 of Handbook]

THERMAL PROPERTIES

Additional thermal-conductivity data on beryllium oxide (BeO)[566,571] are compared in Figure 12 with the best-fit curve derived from 18 other references given in the Handbook. Data from Reference (566) show a higher thermal conductivity between 72 and 1000 F than has been indicated by other investigators.

Linear-thermal-expansion data from Fitzsimmons[571] for high-purity BeO are in agreement with data in the Handbook. Fitzsimmons' specimens, 1/4 x 1/4 x 2-1/2 inches and about 92 per cent dense, were prepared from UOX beryllium oxide powder. Linear expansion was measured by optical apparatus.
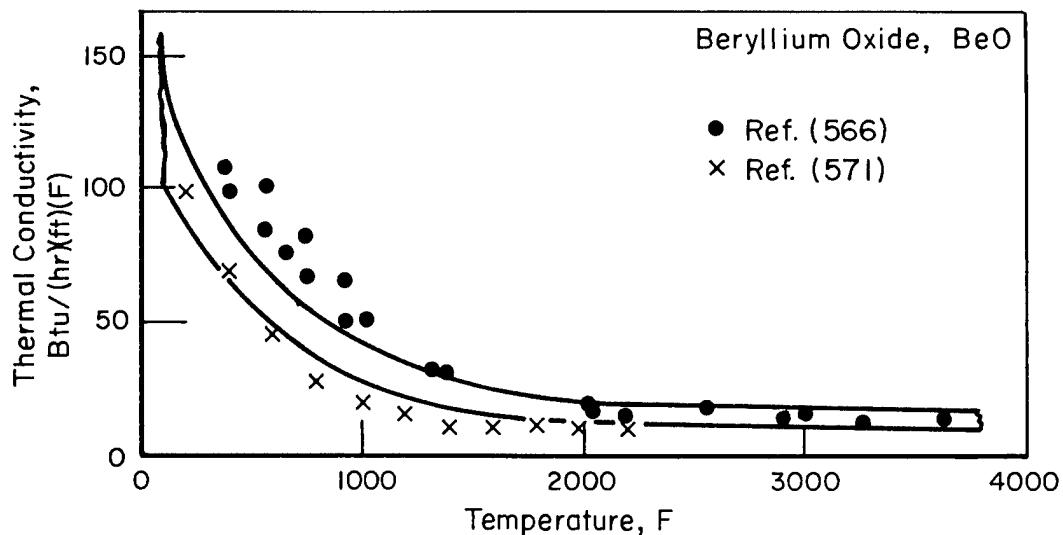
FIGURE 12. THERMAL CONDUCTIVITY OF BERYLLIUM OXIDE

Reference	Reference Information
(566)	Hot pressed, hollow, cylindrical specimens, with densities of 98 per cent or higher and purity of 99 per cent or better. Radial-heat-flow apparatus was used for tests.
(571)	Specimens, 1/2 x 1/2 x 7/8 inch and 96 to 97 per cent dense were evaluated by comparative method of Francl and Kingery.

MECHANICAL PROPERTIES

ᵊnd Strength

Bend strengths of 35,000 to 37,000 psi (75 F) and 15,000 to 19,000 psi (2200 to 2900 F) were measured for high-density beryllium oxide.(586) Specimens of high-purity BeO with 1 per cent of MgO were hot pressed to a density 99. 7 per cent of theoretical and the grain size range was 10 to 100 microns. No test conditions were given.

Compressive-strength data on high-purity beryllia reported by Pratt and Whitney(566) coincide with the best-fit curve in the Handbook. Values for specimens of hot-pressed BeO, 98 per cent dense, and pressed-sintered BeO, 93-95 per cent dense, were 240,000 to 295,000 psi at room temperature, decreasing to 20,000 psi at about 2200 F.

MAGNESIUM OXIDE

[See pages 227-234 of Handbook]

MECHANICAL PROPERTIES
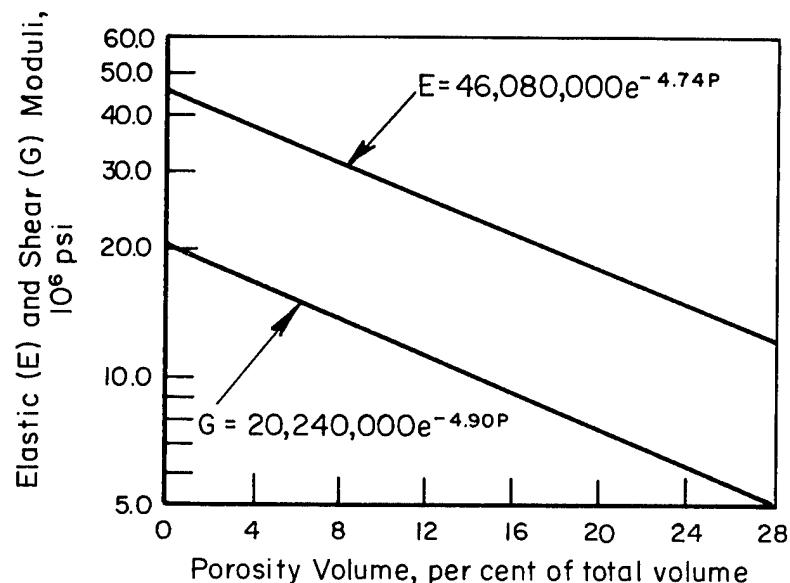
FIGURE 13. EFFECT OF POROSITY ON ELASTIC AND SHEAR MODULI
OF POLYCRYSTALLINE MAGNESIUM OXIDE[607]

Curves represent compilation of moduli data from
various investigators.

OXIDES OF ZIRCONIUM AND HAFNIUM

[See pages 239-246 of Handbook]

THERMAL PROPERTIES

TABLE 18. AVERAGE LINEAR THERMAL EXPANSION
COEFFICIENT FOR ZIRCONIA
(YTTRIA STABILIZED)[571]

Temperature Range, F	Linear Thermal Expansion Coefficient[a], $10^{-6}/F$	
	$ZrO_2-12Y_2O_3$[b]	$ZrO_2-15Y_2O_3$[b]
77-212	3.91	4.18
77-572	4.02	4.57
77-932	4.21	4.92
77-1472	4.39	5.22
77-2012	4.88	5.62
77-2552	5.41	5.92
77-2822	5.64	6.12

(a) $ZrO_2-12Y_2O_3$ sintered at 3000 F for 2 hours in hydrogen; 97.2 per cent dense.
    $ZrO_2-15Y_2O_3$ sintered at 3100 F for 2 hours in air; 86.7 per cent dense.
(b) Composition in weight per cent.

TABLE 19. THERMAL CONDUCTIVITY OF ZIRCONIA
(YTTRIA STABILIZED)[571]

Temperature, F	Thermal Conductivity $(ZrO_2-15Y_2O_3)$[a] Btu/(hr)(ft)(F)
400	0.88
800	0.90
1200	0.92
1600	0.94
2000	0.96

(a) Sintered at 3100 F for 2 hours in air; 86.7 per cent dense.
    Composition is in weight per cent.

OXIDES OF THE RARE-EARTH METALS

[See pages 255-258 of Handbook]

THERMAL PROPERTIES
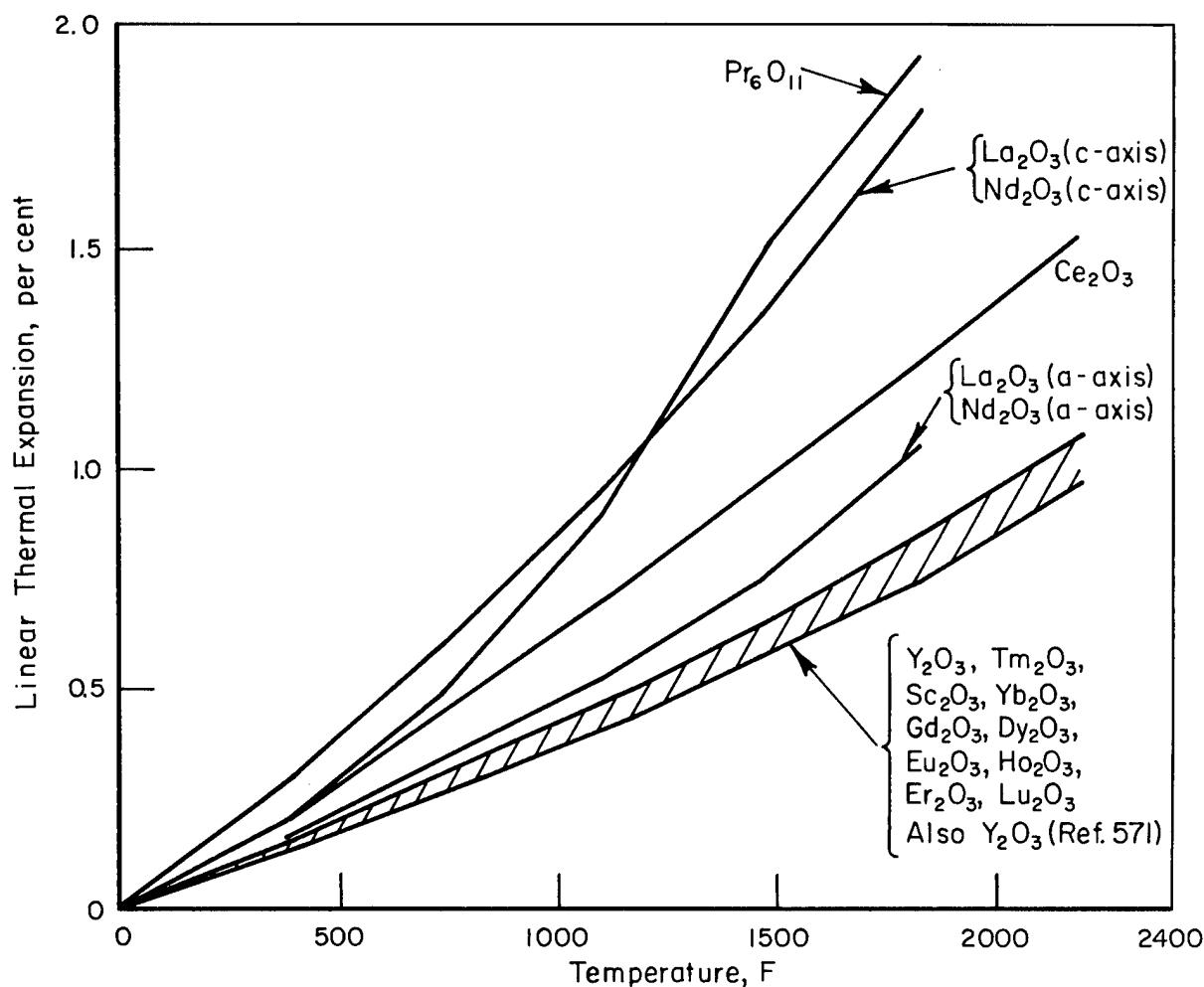
FIGURE 14.   LINEAR THERMAL EXPANSION OF RARE-EARTH OXIDES[608]

Calculated from X-ray diffraction measurements; high-purity
materials obtained from commercial sources and sintered
prior to X-ray examinations.

THERMAL PROPERTIES (Continued)

TABLE 20. THERMAL CONDUCTIVITY OF
YTTRIUM OXIDE (Y_2O_3)[571]

Temperature, F	Thermal Conductivity[a], Btu/(hr)(ft)(F)
200	7.99
400	6.05
800	3.10
1200	2.06
1600	1.76
2000	1.57

(a) Comparative method by Francl and Kingery; specimens
were 1/2 x 1/2 x 7/8 inch and 96.3 per cent dense. Data
are not corrected for porosity.

OTHER PROPERTIES

Corrosion Resistance

Europium oxide, Eu_2O_3, had greater resistance to attack by boiling water than did samarium oxide, Sm_2O_3; specimens of both oxides had densities greater than 90 per cent of theoretical.[606]

OXIDES OF THORIUM, URANIUM, AND PLUTONIUM

[See pages 259-270 of Handbook]

THERMAL PROPERTIES

Information from the following references substantiate the thermal-property data for UO_2 and ThO_2 which are given in the Handbook.

Reference	Property	Reference Information
(587)	Thermal conductivity	Pressed and sintered UO_2; 93.4 per cent of theoretical density. Measurements by radial-heat-flow apparatus (80-1600 F).
(618)	Linear thermal expansion	Pressed and sintered ThO_2; 96 per cent of theoretical density, measurements by interferometric techniques up to 1500 F.

SILICATES

[See pages 279-284 of Handbook]

PHYSICAL PROPERTIES

TABLE 21. PHYSICAL PROPERTIES OF SILICATES

Silicate	Density[a], g/cm^3	Melting Temperature, F	References
$Sc_2O_3 \cdot SiO_2$	3.49[a]	3542	(612,613)
$Sc_2O_3 \cdot 2SiO_2$	3.39[a]	3380	(612,613)
$Pr_2O_3 \cdot SiO_2$	--	(b)	(577)
$2Pr_2O_3 \cdot 3SiO_2$	--	(c)	(577)
$Pr_2O_3 \cdot 2SiO_2$	--	(c)	(577)
$Y_2O_3 \cdot SiO_2 \cdot$	4.32	3500	(576)
$2Y_2O_3 \cdot 3SiO_2$	--	--	(611)
$Y_2O_3 \cdot 2SiO_2$	--	--	(611)

(a) Pycnometer density.
(b) Unstable above 2550 F.
(c) Formed above 2550 F.

OTHER MIXED OXIDES

[See pages 291-297 of Handbook]

PHYSICAL PROPERTIES

TABLE 22. PHYSICAL PROPERTIES OF MIXED OXIDES

Compound	Formula	Crystal Structure	Density, g/cm^3	Melting Temperature, F	References
Aluminum niobate	$AlNbO_4$[a]	Modified tetragonal	--	~2820	(591)
Calcium niobate	$CaO \cdot Nb_2O_5$	--	--	2840	(575)
	$2CaO \cdot Nb_2O_5$	--	--	2865	(575)
	$3CaO \cdot Nb_2O_5$	Cubic	4.23[b]	2840	(575)
Magnesium germanate	$MgO \cdot GeO_2$	Orthorhombic	--	3092	(599)
	$2MgO \cdot GeO_2$	(c)	--	3372	(599)
	$4MgO \cdot GeO_2$	Hexagonal	--	3723[d]	(599)
Hafnium titanate	$HfO_2 \cdot TiO_2$	Orthorhombic	7.21[e]	--	(573)

(a) An intermediate compound in the Al_2O_3-Nb_2O_3 system.
(b) Pycnometer density.
(c) Indicated to have both spinel and olivine structures.
(d) Dissociates to $2MgO \cdot GeO_2$ + MgO.
(e) X-ray density; X-ray pattern similar to $ZrO_2 \cdot TiO_2$.

SULFIDES

[See pages 301-304 of Handbook]

TABLE 23. PHYSICAL, THERMAL, AND MECHANICAL PROPERTIES
OF MONOSULFIDES OF URANIUM AND THORIUM[605]

Properties	Sulfides[a]	
	US	ThS
Temperature of Ignition in Air, F	707	932
Coefficient of Linear Thermal Expansion (32-1800 F), $10^{-6}/F$	6.6	5.7
Bend Strength, 10^3 psi	10-25	16-31
Microhardness (VHN), kg/mm^2	162-276	219-246

(a) Pressed and sintered specimens, 85 to 90 per cent of theoretical density.

ALUMINIDES AND BERYLLIDES

[See pages 307-312 and 315-343 of Handbook]

TABLE 24. DENSITY, HARDNESS, AND OXIDATION RESISTANCE OF THORIUM ALUMINIDE (Th_2Al) AND THORIUM BERYLLIDE ($ThBe_{13}$)[568]

	Th_2Al[a]	$ThBe_{13}$[a]
X-Ray Density, g/cm^3	9.67	4.10
Knoop Hardness (100-G Load) at Room Temperature, kg/mm^2	454	1343
Oxidation Resistance at 1100 F as Weight Gain, $mg/(cm^2)(hr)$		
Flowing dry air	145	0.02
Flowing CO_2	200	0.05

(a) Arc-melted and cast specimens.

SILICIDES OF TITANIUM, ZIRCONIUM, AND HAFNIUM

[See pages 351-354 of Handbook]

THERMAL PROPERTIES

TABLE 25. COEFFICIENT OF LINEAR THERMAL EXPANSION OF TITANIUM SILICIDES[592]

Silicide[a]	Temperature Range, F	Thermal-Expansion Coefficient, 10^{-6}/F
Ti_5Si_3	338-1958	6.1
TiSi	68-698	4.9
	698-1958	5.8
$TiSi_2$	68-1958	5.8

(a) Hot-pressed specimens, 90-95 per cent dense, containing 0.3 to 0.5 per cent free silicon; dilatometer apparatus.

SILICIDES OF VANADIUM, NIOBIUM, AND TANTALUM

[See pages 355-358 of Handbook]

THERMAL PROPERTIES

TABLE 26. COEFFICIENT OF LINEAR THERMAL EXPANSION OF SILICIDES OF VANADIUM, NIOBIUM, AND TANTALUM[592]

Silicide[a]	Temperature Range, F	Thermal-Expansion Coefficient, 10^{-6}/F
V_3Si	68-1148	4.4
	1148-1508	6.6
	1508-1958	7.8
V_5Si_3	68-1418	5.3
	1418-1958	6.2
VSi_2	68-1418	6.2
	1418-1958	8.2
$NbSi_2$	68-698	4.7
	698-1958	6.5
$TaSi_2$	68-608	5.3
	608-1958	6.0

(a) Hot-pressed specimens, 90-95 per cent dense, containing 0.3 to 0.5 per cent free silicon; dilatometer apparatus.

SILICIDES OF CHROMIUM, MOLYBDENUM, AND TUNGSTEN

[See pages 359-368 of Handbook]

THERMAL PROPERTIES

TABLE 27. COEFFICIENT OF LINEAR THERMAL EXPANSION OF SILICIDES OF CHROMIUM, MOLYBDENUM, AND TUNGSTEN[592]

Silicide[a]	Temperature Range, F	Thermal-Expansion Coefficient, 10^{-6}/F
Cr_3Si	68-1958	5.8
Cr_5Si_3	68-338	3.3
	338-1328	5.9
	1328-1958	7.9
$CrSi$	68-1418	6.3
Mo_3Si	68-338	1.9
	338-1958	3.6
Mo_5Si_3	68-518	2.4
	518-1958	4.1
$MoSi_2$	68-1958	4.6
WSi_2	68-788	3.5
	788-1958	4.4

(a) Hot-pressed specimens, 90-95 per cent dense, containing 0.3 to 0 5 per cent free silicon; dilatometer apparatus.

MECHANICAL PROPERTIES
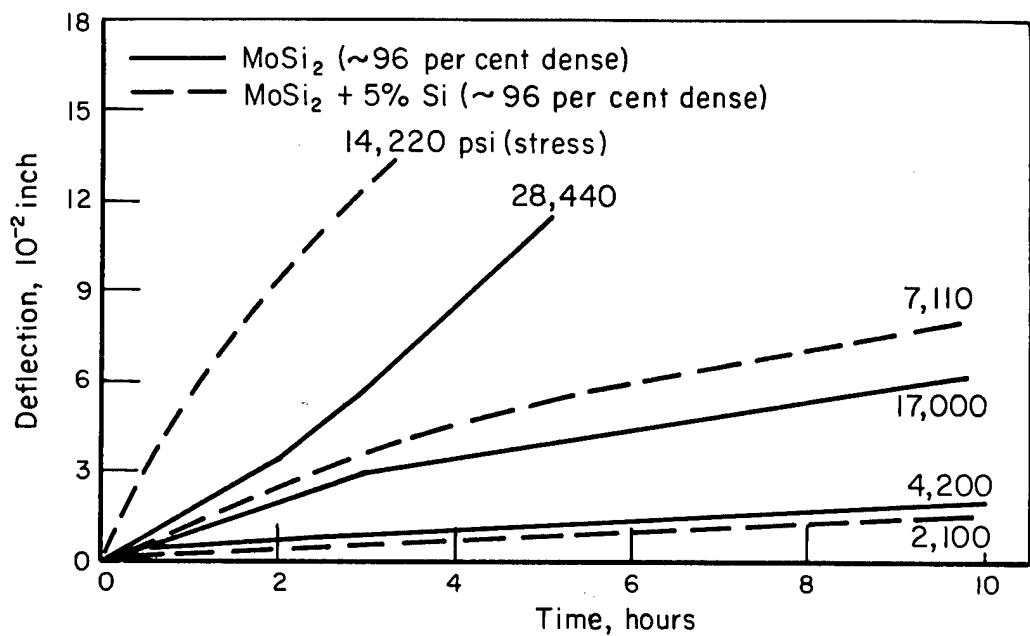
FIGURE 15. BEND CREEP OF MOLYBDENUM DISILICIDE AT 2200 F[561]
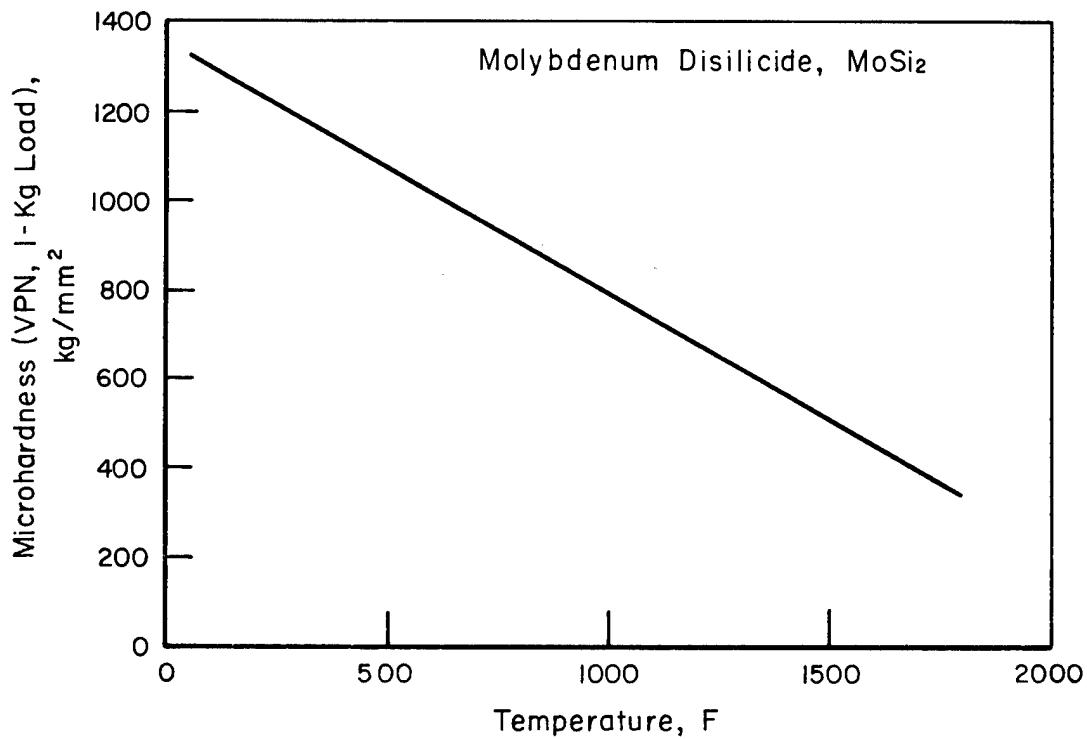
FIGURE 16. EFFECT OF TEMPERATURE ON MICROHARDNESS
OF MOLYBDENUM DISILICIDE[561]

SILICIDES OF RARE-EARTH METALS

[See pages 369-370 of Handbook]

PHYSICAL PROPERTIES

TABLE 28.   CRYSTAL STRUCTURE OF RARE-
EARTH SILICIDES[583]

Silicide	Crystal Structure
Y_3Si_5	Orthorhombic
Gd_3Si_5	Orthorhombic
Dy_3Si_5	Orthorhombic
Er_3Si_5	Hexagonal
Lu_3Si_5	Hexagonal

THERMAL PROPERTIES

Coefficients of linear thermal expansion of lanthanium disilicide ($LaSi_2$) were reported to be 4.3×10^{-6}/F (68-608 F) and 5.95×10^{-6}/F (608-1958 F)[592]. Specimens were hot-pressed to 90 to 95 per cent dense and contained 0.3 to 0.5 per cent free silicon. A dilatometer apparatus was used.

SILICIDES OF THORIUM, URANIUM, AND PLUTONIUM

[See pages 371-374 of Handbook]

TABLE 29. DENSITY, HARDNESS, AND OXIDATION RESISTANCE
OF THE THORIUM SILICIDES Th_3Si_2 AND ThSi[568]

	Th_3Si_2[a]	ThSi[a]
X-Ray Density, g/cm^3	9.81	8.99
Knoop Hardness (100-G Load) at Room Temperature, kg/mm^2	825	696
Oxidation Resistance at 1100 F as Weight Gain, $mg/(cm^2)(hr)$		
Flowing Dry Air	595	265
Flowing CO_2	512	459

(a) Arc-melted and cast specimens.

OTHER SILICIDES

[See pages 375-376 of Handbook]

(Compounds designated boron silicides are also termed silicon borides in the literature.)

PHYSICAL PROPERTIES

Studies by Finnie[570] on the structures and compositions of the silicides of ruthenium, osmium, rhodium, and iridium substantiate information already included in the Handbook.

Pycnometer densities of B_4Si and B_6Si were 2.47 ± 0.02 and 2.44 ± 0.02 g/cm^3.[569]

THERMAL PROPERTIES

Coefficient of linear thermal expansion of rhenium disilicide ($ReSi_2$) for the temperature range of 68 to 1958 F was reported to be $3.67 \times 10^{-6}/F$.[592]

The thermal conductivity and linear thermal expansion of B_4Si and B_6Si are shown on the following page in Figure 17.[569]

MECHANICAL PROPERTIES

Bend strengths at room temperature of B_4Si and B_6Si were 8,000 to 11,000 psi and 20,000 to 24,000 psi, respectively. Young's moduli of 30 to 40×10^6 psi were calculated for the nonporous boron silicides from data on porous specimens[569]. For bend strength and modulus measurements, specimens were about 0.1 x 0.2 x 0.75 inch. The porosity of B_4Si was about 6 per cent and of B_6Si about 15 per cent.

Average microhardnesses were 2000 and 2350 kg/mm^2 for B_4Si and B_6Si, respectively, at room temperature.[569]
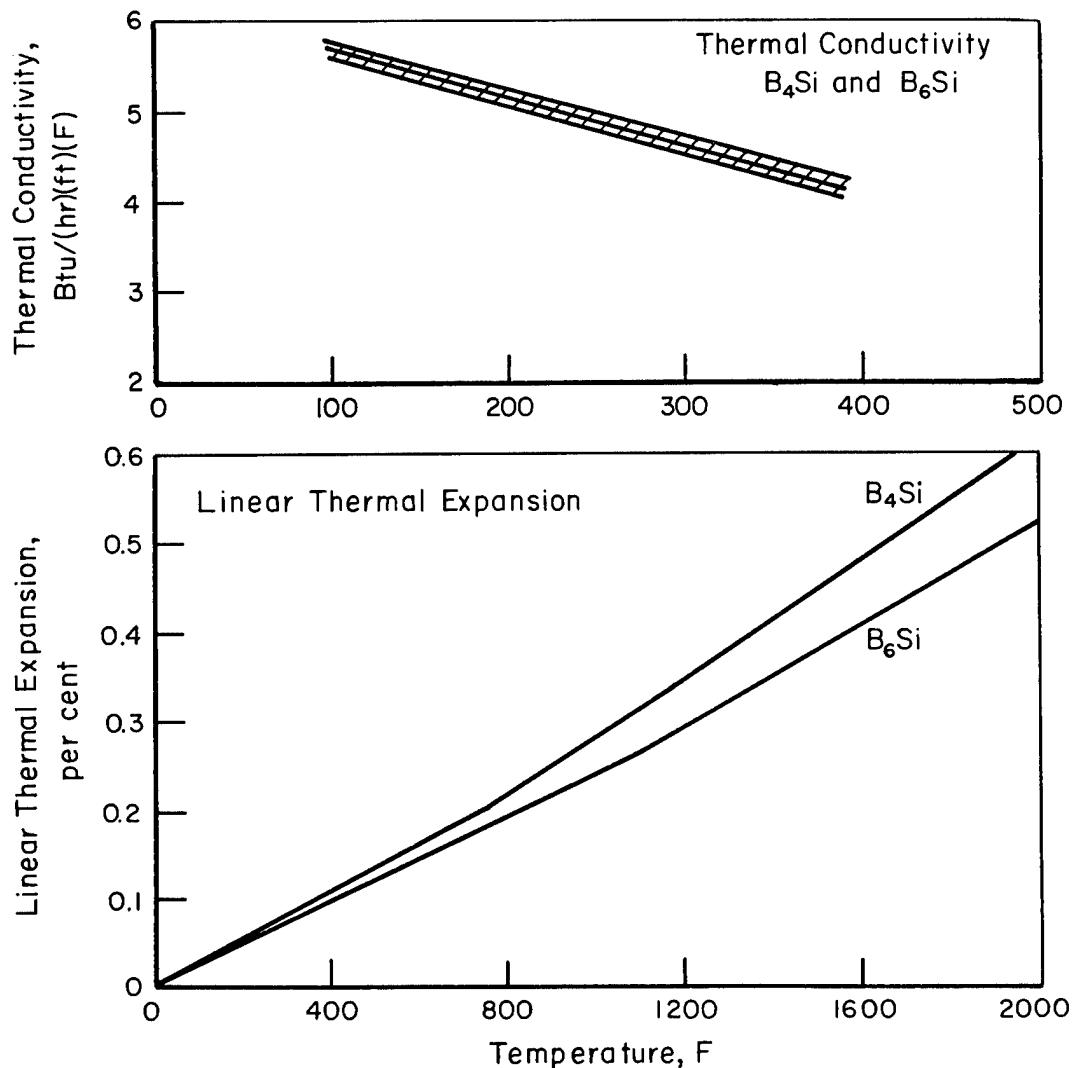
FIGURE 17.   THERMAL CONDUCTIVITY AND LINEAR THERMAL EXPANSION OF
BORON SILICIDES AT ZERO POROSITY[569]

Thermal conductivity specimens were 0. 5 x 0. 5 x 0. 825 inch; B_4Si
79. 8 per cent dense, B_6Si 85. 8 per cent dense; comparative
method of Francl and Kingery.

Thermal expansion specimens were 0. 14-inch diameter and 0. 5
to 1. 25 inches long; B_4Si 85. 3 per cent dense, B_6Si 93. 9 per
cent dense; dilatometer measurements.

OTHER PROPERTIES

Oxidation Resistance
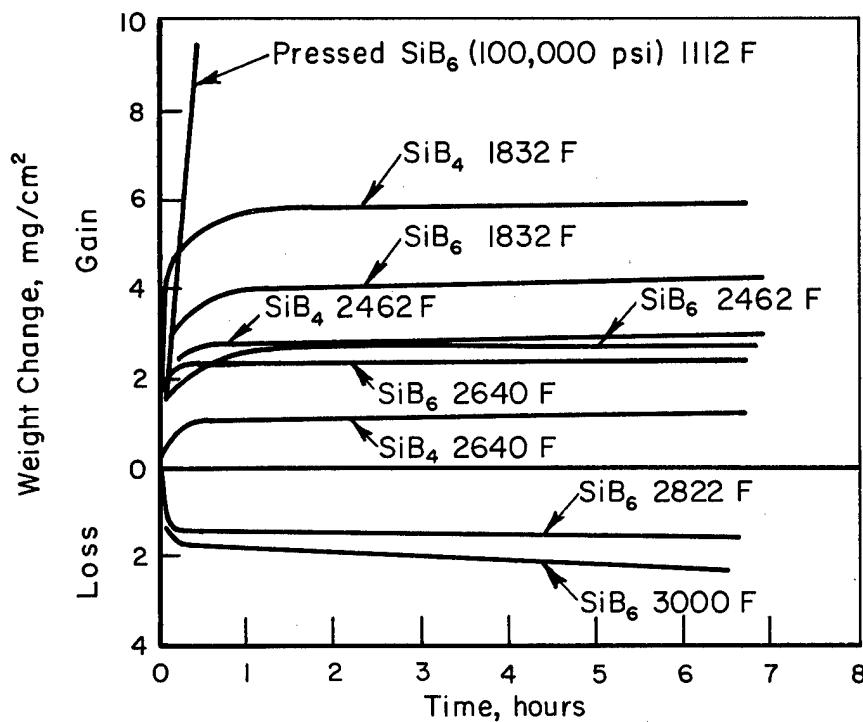
FIGURE 18. WEIGHT CHANGE OF BORON SILICIDES IN AIR AS A
FUNCTION OF TIME[569]

OTHER INTERMETALLIC COMPOUNDS

[See pages 379-382 of Handbook]

PHYSICAL PROPERTIES

TABLE 30.   PHYSICAL PROPERTIES OF OTHER INTERMETALLIC COMPOUNDS

System	Compound Formula	Crystal Structure	Melting Point, F	References
Cerium-selenium	CeSe	Cubic	~3300	(589)
	Ce_2Se_3	Cubic	2900-3720[a]	(590)
Cerium-tellurium	CeTe	Cubic	2890-3430[a]	(589)
	Ce_2Te_3	Cubic	3030-3270[a]	(589)
Erbium-selenium	Er_2Se_3	--	~2768	(590)
Gadolinium-selenium	GdSe	Cubic	3385	(589)
Gadolinium-tellurium	GdTe	Cubic	3400	(589)
Neodymium-tellurium	NdTe	Cubic	3710	(589)
	Nd_3Te_4	Cubic	3060	(589)
Niobium-tellurium	NbTe	Cubic	3000	(589)
Samarium-selenium	SmSe	Cubic	~3800	(589)
Samarium-tellurium	SmTe	Cubic	3480	(589)
Ytterbium-selenium	YbSe	Cubic	3530	(589)
Ytterbium-tellurium	YbTe	Cubic	3160	(589)
Yttrium-tellurium	Y_2Te_3	Cubic	2777	(590)
Niobium-phosphorus	NbP[b]	--	3146	(600,572)
Titanium-phosphorus	TiP[c]	--	2846	(600,572)
Tantalum-phosphorus	TaP[d]	--	3020	(600,572)

(a) Not resolved.
(b) X-ray density 6.54 g/cm^3.
(c) X-ray density 4.27 g/cm^3.
(d) X-ray density 11.15 g/cm^3.

MECHANICAL PROPERTIES

TABLE 31. MICROHARDNESS OF TRANSITION-METAL
PHOSPHIDES[600]

Phosphide[a]	Average Microhardness (DPH, 17-G Load), kg/mm^2
TiP	718
NbP	599
TaP	374

(a) Powder samples mounted in resin.

OTHER PROPERTIES

Oxidation Resistance

Oxidation resistance of the phosphides is a function of the composition and state
of the oxidation product. Weight gains were 1 per cent in TiP, NbP, and TaP powders
(100 mesh) heated at 1058, 1328, and 1616 F, respectively. A weight loss occurred
at slightly higher temperatures because of volatilization of oxidation products.[600]

REFERENCES

561. Brokhin, I. S., Zolotarev, I. S., and Baranov, A. I., "Production and Properties of Molybdenum Disilicide", Sbornik Trudov. Vsesoiuznyi Nauchno-Issledovatel'skii Institut Tverdykh (2), 24-36 (1960).

562. Brown, D. J., and Stobo, J. J., "Preparation and Properties of Uranium Monocarbide", Plansee Proceedings, 4th Seminar, 1961, Reutte/Tyrol, 279-293 (1962).

563. Crandall, W. B., Chung, D. H., and Gray, T. J., "Mechanical Properties Ultra-Fine Hot-Pressed Alumina", Mechanical Properties of Engineering Ceramics, Proceedings, 349-379 (1961).

564. Deeley, G. G., Herbert, J. M., and Moore, N. C., "Dense Silicon Nitride", Powder Metallurgy, 8, 145-151 (1961).

565. Eckstein, B. H., and Forman, R., "Preparation and Some Properties of Tantalum Carbide", Journal of Applied Physics, 33, 82-87 (1962).

566. Emanuelson, R. C., Pratt & Whitney Aircraft Company, "Electrical, Mechanical & Thermal Properties of Hot Pressed and Sintered BeO", Supplement No. 1, APR-1048 (June 12, 1963).

567. Engelke, J. L., Halden, F. A., and Farley, E. P., "Synthesis of New High-Temperature Materials", U. S. Department of Commerce, Office of Technical Service, PB-161,720 (1960).

568. Farkas, M. S., Bauer, A. A., and Dickerson, R. F., Battelle Memorial Institute, "Evaluation of Thorium and Thorium-Uranium Compounds as Thermal Breeder Fuels", BMI-1568 (February 15, 1962).

569. Feigelson, R. S., Watertown Arsenal Laboratories, "Some Physical Properties of Polycrystalline Silicon Boride", Technical Report, WAL-TR-853-1 (May 1962).

570. Finnie, L. N., "Structures and Compositions of the Silicides of Ruthenium, Osmium, Rhodium and Iridium", Journal of the Less-Common Metals, 4, 24-34 (1962).

571. Fitzsimmons, E. S., General Electric Company, Aircraft Nuclear Propulsion Department, "Summary of Thermal Expansion and Thermal Conductivity Measurements by Lexington Laboratories", DC-61-6-4, Contract AT(11-1)-171 (May 1961).

572. Gingerich, K. A., Pennsylvania State University, "A Study of High Temperature Properties of Titanium and Zirconium Phosphides and Related Refractory Materials. Progress Report for the Period January 1, 1961 to December 31, 1961", TID-14770, Contract AT(30-1)-2541 (January 1962).

573. Godina, N. A., Keler, E. K., and Rudenko, V. S., "Interaction of Hafnium Dioxide With Titanium Dioxide", Zhurnal Neorganicheskoi Khimii, 5, 2795-2797 (1960).

574. Rare Earth Research, Gordon and Breach Science Publishers, New York (1962), "Rare-Earth Borides for Nuclear Application" (E. W. Hoyt), pp. 287-299.

575. Ibrahim, M., Bright, N. F. H., and Rowland, J. F., "The Binary System CaO-Nb$_2$O$_5$", American Ceramic Society, Journal, 45, 329-334 (July 1962).

576. Keler, E. K., and Kuznetsov, A. K., "The Preparation and Physical Properties of Yttrium Oxyorthosilicate Y$_2$O(SiO$_4$)", Zhurnal Prikladnoi Khimii, 35, 250-256 (February 1962).

577. Keler, E. K., Godina, N. A., and Savchenko, E. P., "The Reactions Between Silica and Praseodymium Oxide in Solid Phases", Izvestiia Akademii Nauk SSSR, Otdelenie Khimicheskikh Nauk (10), 1735-1741 (October 1961).

578. Keller, D. L., "The Development of Uranium Mononitride", report to Thirteenth High Temperature Fuels Committee Meeting, Palo Alto, California, Contract W-7405-eng-92 (December 1961).

579. Kempter, C. P., and Krikorian, N. H., "Some Properties of Thorium Monocarbide and Dicarbide", Journal of the Less-Common Metals, 4, 244-251 (1962).

580. Kharchenko, V. K., and Struk, L. I., "Certain Data on the Effect of Temperature on the Strength and Plasticity of Some Refractory Compounds", Poroshkovaya Met. (2), 87-91 (March-April 1962).

581. Knudsen, F. P., "Effect of Porosity on Young's Modulus of Alumina", American Ceramic Society, Journal, 45 (2), 94-95 (1962).

582. Kruger, O. L., Argonne National Laboratory, Metallurgy Branch, "Properties of PuC", Annual Report, ANL-6330, Contract W-31-109-eng-38 (1960), pp. 82-90.

583. Rare Earth Research, Macmillan Company, New York (1961), "A Structural Survey of the Heavy Rare Earth Silicides" (C. E. Lundin), pp. 306-313.

584. Lvov, S. N., Nemchenko, V. F., and Samsonov, G. V., "Heat Conduction of Refractory Borides, Carbides and Nitrides", Poroshkovaya Met. (6), 70-74 (1961).

585. McClelland, J. D., and Petersen, L. O., "The Effect of Porosity on the Thermal Conductivity of Alumina", U. S. Atomic Energy Commission, NAA-SR-6473 (1961).

586. McClelland, J. D., Richardson, J. H., and Franklin, L. R., "Fabrication and Properties of Translucent Beryllium Oxide", U. S. Atomic Energy Commission, NAA-SR-6454 (1961).

587. McHargue, C. J., Oak Ridge National Laboratory, Metals and Ceramics Division, "IV. Applied Research", Annual Progress Report for period ending May 31, 1962, ORNL-3313, pp. 133-178.

588. Marchal, M., and Trouve, J., "Study of the System Carbon-Uranium-Thorium", Commissariat a l'Energie Atomique, Centre d'Etudes Nucleaires, Saclay, Quarterly Progress Report No. 4, (October 1-December 31, 1961), Translated by Monks, A. L., Oak Ridge National Laboratory, CEA-3677 (January 10, 1962).

589. Rare Earth Research, Gordon and Breach Science Publishers, New York (1962), "Studies on the Selenides and Tellurides of Selected Rare-Earth Metals" (J. F. Miller, L. K. Matson, and R. C. Himes), pp. 233-248.

590. Rare Earth Research, Macmillan Company, New York (1961), "Rare Earth Intermetallic Compounds With Elements of Groups V and VI" (J. F. Miller and R. C. Himes), pp. 232-240.

591. Mueller, E. K., and Nicholson, B. J., "Concerning the Phase Diagram and Dielectric Behavior of the Oxide System", American Ceramic Society, Journal, 45, 250-251 (May 1962).

592. Neshpor, V. S., and Reznichenko, M. I., "Investigating the Thermal Expansion of Some Silicides", Ogneupory (3), 134-137 (March 1963).

593. Nowotny, H., Benesovsky, F., and Kieffer, R., "The Systems Nb-B and Ta-B", Zeitschrift fur Metallkunde, 50, 417-423 (1959).

594. Pallmer, P. G., General Electric Company, Hanford Atomic Products Operation, "Thermal Expansion of Plutonium Carbides", HW-72245, Contract AT(45-1)-1350 (February 1962).

595. Parr, N. L., Sands, R., Pratt, P. L., May, E. R. W., Shakespeare, C. R., and Thompson, D. S., "Structural Aspects of Silicon Nitride", Powder Metallurgy, 8, 152-163 (1961).

596. Peakall, K. A., and Antill, J. E., "Oxidation of Uranium Monocarbide", Journal of the Less-Common Metals, 4, 426-435 (1962).

597. Popper, P., and Ruddlesden, S. N., "The Preparation, Properties, and Structure of Silicon Nitride", British Ceramic Society, Transactions, 60, 603-626 (1961).

598. Pratt, P. L., "Microstructure and Mechanical Properties of Silicon Nitride", Mechanical Properties of Engineering Ceramics, Proceedings, 507-519 (1961).

599. Robbins, C. R., and Levin, E. M., "System Magnesium Oxide-Germanium Dioxide", American Journal of Science, 257 (1), 63-70 (1959).

600. Ripley, R. L., "The Preparation and Properties of Some Transition Phosphides", Journal of the Less-Common Metals, 4, 496-503 (1962).

601. Samsonov, G. V., Kosolapova, T. Ya., and Makarenko, G. N., "Preparation and Physico-Chemical Properties of Yttrium Carbides", Zhurnal Neorganicheskoi Khimii, 7, 975-979 (May 1962).

602. Samsonov, G. V., Makarenko, G. N., and Kosolapova, T. Ya., "Scandium Carbides and Compound Scandium-Titanium Carbides", Akademiia Nauk SSSR, Doklady, 144, 1062-1065 (1962).

603. Samsonov, G. V., Serebryakova, T. I., and Bolgar, A. S., "Preparation and Physico-Chemical Properties of Strontium Hexaboride", Zhurnal Neorganicheskoi Khimii, 6, 2243-2248 (October 1961).

604. Samsonov, G. V., and Verkhoglyadova, T. S., "Hardness of Transition Metal Nitrides", Zhurnal Strukturnoi Khimii, 2, 617-618 (September-October 1961).

605. Shalek, P. D., "Fabrication and Properties of US and ThS Bodies", American Nuclear Society, Transactions, 5 (1), 244-245 (June 1962).

606. Shears, E. C., "Samarium and Europium Oxalates, Oxides, and Their Hydrates", British Ceramic Society, Transactions, 61 (5), 225-245 (1962).

607. Spriggs, R. M., Brissette, L. A., and Vasilos, T., "Effect of Porosity on Elastic and Shear Moduli of Polycrystalline Magnesium Oxide", American Ceramic Society, Journal, 45 (8), 400 (1962).

608. Stecura, S., and Campbell, W. J., "Thermal Expansion and Phase Inversion of Rare-Earth Oxides", U. S. Bureau of Mines Report of Investigations 5847 (1961), 47 pp.

609. Taylor, R. E., "Thermal Conductivity of Zirconium Carbide at High Temperatures", American Ceramic Society, Journal, 45, 353-354 (July 1962).

610. Taylor, K. M., and McMurtry, C. H., Carborundum Company, "Synthesis and Fabrication of Refractory Uranium Compounds", ORO-400, Contract AT(40-1)-2558 (February 1961).

611. Toropov, N. A., and Bondar, I. A., "Silicates of the Rare-Earth Elements. Communication 3. Phase Diagram of the Binary System Yttrium Oxide-Silica", Izvestiia Akademii Nauk S.S.S.R., Otdelenie Khimicheskikh Nauk, 4, 544 (1961).

612. Toropov, N. A., and Vasil'eva, V. A., "Synthetic Scandium Silicates", Soviet Phys.-Cryst., 6, 779-783 (May-June 1962).

613. Toropov, N. A., and Vasil'eva, V. A., "Equilibrium Diagram of the Scandium Oxide-Silica Binary System", Russian Journal of Inorganic Chemistry, 7 (8), 1001-1005 (August 1962).

614. Vekshina, N. V., and Markovskii, L. Ya., "Chemical Properties of Hexaborides of Alkaline Earth Metals", Zhurnal Prikladnoi Khimii, 34, 2171-2175 (1961).

615. Yavorsky, P. J., "Properties and High Temperature Applications of Zirconium Oxide", Ceramic Age, 78 (6), 64-66, 68-69 (1962).

616. Yerkovich, L. A., and Kirchner, H. P., Cornell Aeronautical Laboratory, Inc., "Growth and Mechanical Properties of Filamentary Silicon Carbide Crystals", WADD-TR-61-252 (August 1961).

617. Zhuravlev, N. N., Stepanova, A. A., Paderno, Yu. B., and Samsonov, G. V., "Determination of the Coefficient of Thermal Expansion of Hexaborides by X-Ray Analysis", Kristallografiia, 6, 791-794 (1961).

618. Wachtman, J. B., Jr., Scuderi, T. G., and Cleek, G. W., "Linear Thermal Expansion of Aluminum Oxide and Thorium Oxide From 100° to $1100^{\circ}K$", American Ceramic Society, Journal, 45, 319-323 (July 1962).

APPENDIX

A CRITICAL DISCUSSION OF ANALYTICAL TECHNIQUES
FOR DESCRIBING THE STRENGTH CHARACTERISTICS
OF BRITTLE MATERIALS

Introduction

Appendix A of the Materials Selection Handbook (RTD-TDR-63-4102) contains a discussion of the weakest-link model for describing the fracture-strength characteristics of brittle materials. The Weibull mathematical treatment of the weakest-link model is discussed in particular, as it is the most widely accepted of the various treatments that have been proposed. The discussion in the Handbook was purposely brief for two reasons. First, no one model of brittle fracture, much less any one specific mathematical treatment, has been sufficiently verified to justify its use as the basis of a rational design philosophy. Second, the objective of the discussion was to provide guidelines for design approaches with brittle materials rather than to review all available concepts.

The Weibull theory is receiving increasing attention as a design tool. It is being used to calculate design stress values having low fracture probabilities for application to complex-stress conditions from limited laboratory test data obtained under simple-stress conditions. Although the cautious use of the Weibull theory for limited extrapolations may be warranted in certain cases, its use as a quantitative law of general applicability is not presently justified.

In an attempt to avoid its misuse, this Supplement will consider some of the limitations of the Weibull approach. Also, other approaches which may be of value will be considered. In keeping with the above-stated purpose of the Handbook — to provide guidelines for design rather than detailed research-type information — no attempt will be made to fully explore all arguments.* Rather, it will be emphasized that the present state of understanding of brittle behavior is not sufficiently advanced to provide a sound basis for evaluating approaches to the design with brittle materials.

Review of Brittle-Fracture Characteristics

It may be helpful to review briefly those factors which distinguish the strength characteristics of brittle materials from those of more conventional, ductile materials. For our purposes, a material can be said to be in a brittle state if its stress-strain curve is essentially linear to fracture; that is, if it has no capacity for inelastic strain. Theoretically, the tensile strength of a material is about 1/10 of its elastic modulus, of the order of millions of psi. Measured strengths are generally 1, 2, or 3 orders of magnitude below this. The difference is ascribed to imperfections in the material. In the case of ductile materials, the movement of dislocations results in yielding (plastic

*More detailed coverage can be found in References (A-1) and (A-2).

flow) at relatively low stresses. For brittle materials, flaws such as microcracks cause stress concentrations which can lead to brittle fracture. It can be shown that microscopic and submicroscopic cracks can, in the absence of ductility, cause stress concentrations on the order of 1000. Thus, local stresses of millions of psi (the theoretical strength) may be associated with nominal stresses of thousands of psi.

The measured quantity in a strength test is the nominal stress at fracture. This can be referred to as the "nominal strength". This nominal strength might be satisfactory for design purposes (since designs are based on nominal stresses*), except for three commonly observed characteristics of brittle materials:

(1) Nominal strengths exhibit a considerable amount of scatter.

(2) The nominal strengths are size dependent (observed strength decreases with increasing specimen size).

(3) The nominal strengths are sensitive to the distribution of nominal stresses in the body (e.g., strengths obtained in bending are higher than those obtained in uniform tension).

It should be noted parenthetically that some doubt has been cast on whether these effects are inherent characteristics of brittle materials or are due to controllable material and testing variables. As an example, the amount of scatter in observed strength values can be reduced by improved control in specimen preparation (from raw material to finishing) and in the testing procedure. The classic example of the size effect is the work of Griffith on glass fibers. This effect was confirmed, at least qualitatively, by several subsequent investigations. More recently, Thomas (A-3) reported studies similar to those of Griffith in which he found no size effect.** In comparing these results with the work of previous investigators, Thomas pointed out that as fiber-drawing techniques were improved, measured strengths increased and the magnitude of the size effect decreased. His strength values, which showed no size effect, were the highest of those included in his discussion. Thomas concluded that the apparent size dependence was not an inherent material property but was associated with fabrication.

These observations, while far from general and conclusive, serve to cast doubt on the validity of any model which assumes scatter, size dependence, and stress-distribution dependence to be inherent characteristics of the strength of brittle materials. Despite this, the weight of evidence now available favors an approach which assumes these effects to be inherent. Let us consider some of the available models for describing the strength characteristics of brittle materials.

Concepts for Describing Brittle-Fracture Characteristics

The models to be considered here will be discussed only in sufficient detail to indicate their qualitative ability to describe the observed behaviors. More detailed treatments can be found in the references cited.

---

*The nominal stresses referred to are those calculated by the best available techniques of stress analysis. They are nominal in the sense that they do not account for the stress concentrations due to the flaws.

**Thomas observed a small decrease in strength with increasing diameter for a group of specimens drawn at a low temperature. He feels that the strength decrease – not observed with specimens drawn at higher temperatures – was associated with poor specimen quality.

Statistical Theories

The statistical approaches relate the characteristics of brittle fracture to the flaws discussed earlier. These flaws are considered to be distributed uniformly throughout the body. Thus, the number of flaws in any unit volume is a constant of the material. However, flaw severity (i.e., the magnitude of the associated stress concentration) is not the same for all flaws; a statistical distribution is used to describe the probability of encountering a flaw of given severity.*

The statistical theories have the very appealing virtue of relating the observed scatter to the size and stress-distribution dependence, thus relating the three character istics of brittle-fracture strength.

Statistical theories can be applied with at least two models: the weakest-link model and the parallel-chain model. The weakest-link model predicts that fracture will initiate at the most highly stressed point in the body. Once fracture is initiated, it will propagate through the body. In terms of a uniformly stressed tension specimen, this predicts that the strength is limited by the single most severe flaw ("weakest link") in the specimen.** The scatter in strength values follows directly, since the severity of the most severe flaw will differ among nominally identical specimens.

The size effect also can be explained by the weakest-link model. Since flaw density is assumed constant, a large specimen will contain a greater number of flaws than will a small specimen. The probability of encountering a flaw of given high severity increases with the number of flaws. Thus, strength would be expected to be inversely related to the specimen size.

The stress-distribution effect can be related to the size effect as follows. Consider two nominally identical specimens, one to be tested in uniform tension, the other in bending. In the case of the tension specimen, the same nominal stress will be applied to each flaw and, as has been noted, the strength will be limited by the single most severe flaw. In the case of the bend specimen, half of the specimen is subjected to compressive stresses. Assuming fracture will not initiate on the compression side of the beam, half of the total number of flaws cannot affect the fracture strength. Further, on the tension side of the beam, the nominal stress varies from zero at the neutral axis to a maximum at the surface. Thus, a severe flaw near the neutral axis may not be as effective in causing fracture as a relatively moderate flaw near the surface. This can be considered as a further reduction in the number of effective flaws. Since there are fewer effective flaws in a bend specimen than in a tension specimen, there is a lower probability of encountering a flaw of given severity. Thus, specimens subjected to bending would be expected to exhibit higher mean fracture strengths than similar specimens subjected to uniform tension.

There are several quantitative treatments of the weakest-link model. Epstein[A-4] pointed out that basically they differ only in the assumed distribution of flaw severities in the parent body. Given this function, the distribution of strengths of a group of specimens taken from the parent body can be found from extreme-value statistics. Epstein noted that available data were not sufficiently sensitive to distinguish among the various proposed distribution functions.

---

*Alternatively, it can be considered that all flaws are of equal severity but that the flaw density is a statistical function.

**The effect of flaw orientation, or course, enters also. This consideration is omitted from the present discussion for simplicity.

Of the various forms of flaw-distribution functions which have been proposed, the Weibull distribution[A-5] is by far the most popular. Two reasons may be cited for this popularity. First, this function provides a reasonably good fit for much of the available data on brittle-fracture strengths. Second, Weibull developed a reasonably complete analytical treatment of the weakest-link problem specifically for application to brittle materials. (Epstein's work, revealing the more general aspects of the problem and pointing out the fact that much of the mathematics had previously been developed, followed Weibull's classic paper by 10 years.)

Weibull makes no claim that his distribution function is anything but empirical. He simply notes that it does provide a reasonable fit to available data and that it is the only function which would make his mathematical derivation tenable. Further consideration of the applicability of the Weibull treatment will be given subsequently.

The other statistical approach, viz., the parallel-chain model, allows the possibility of fracture initiating at a point without propagating. Conceptually, the model consists of a series of chains of equal length arranged in parallel. The strength of such a complex is not governed by the strength of its weakest link. After the weakest link breaks, the chain containing that link can no longer carry the load. The load previously carried by that chain is distributed among the remaining chains. Assuming that they can carry the additional burden, the structure is still intact. A mathematical treatment of the parallel-chain model was developed by Daniels[A-6] for the case of uniaxial tension. The results satisfactorily described strength distributions for bundles of parallel threads.

The parallel-chain model has not been as widely considered as the weakest-link model for application to the brittle-fracture problem. One reason is its relative mathematical complexity. Additionally, the physical picture of independent elements is not intuitively satisfying when considering a solid brittle body. Despite its drawbacks, the parallel-chain model might have limited applicability to the brittle-fracture problem, perhaps in combination with a weakest-link approach.

Nonstatistical Theories

The nonstatistical approaches to brittle fracture assume that the observed size and stress-state dependences can be explained by conventional mechanics. These approaches will not explicitly account for the significant scatter in strength values and, in this sense, are not as satisfying as the statistical theories. As has been noted, however, this scatter may not be an inherent characteristic of the material.

One nonstatistical theory assumes that a skin exists on the surface of the material. This skin is assumed to have a higher strength and higher elastic modulus than the base material. Additionally, it is convenient to assume that the thickness of this skin is independent of the gross dimensions of the body.

If such a body is subjected to an axial tension force, the stress distribution will be as shown in Figure 19. The load carried by the skin is

$$P_{skin} = \sigma_{skin} \cdot A_{skin} \quad .$$
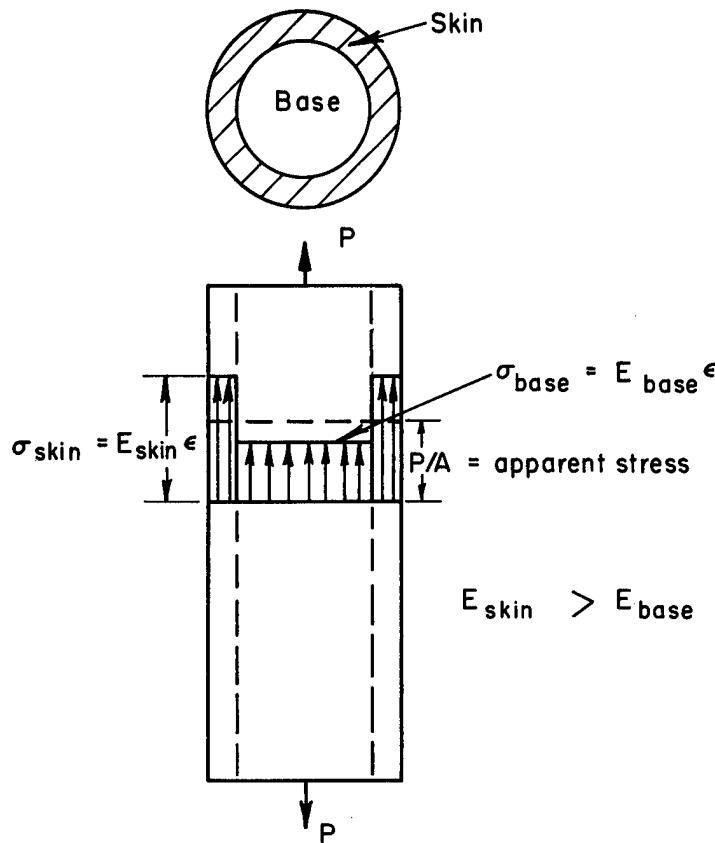
FIGURE 19. STRESS DISTRIBUTION IN A TENSION SPECIMEN
HAVING HIGH-MODULUS SKIN

The load carried by the base material is:

$$P_{base} = \sigma_{base} \cdot A_{base}$$

where   P = load

σ = stress

A = cross-sectional area.

The total load is:

$$P = P_{skin} + P_{base}.$$

The apparent stress on the bonding is:

$$\sigma_{apparent} = P/A = \frac{P_{skin} + P_{base}}{A_{skin} + A_{base}}$$
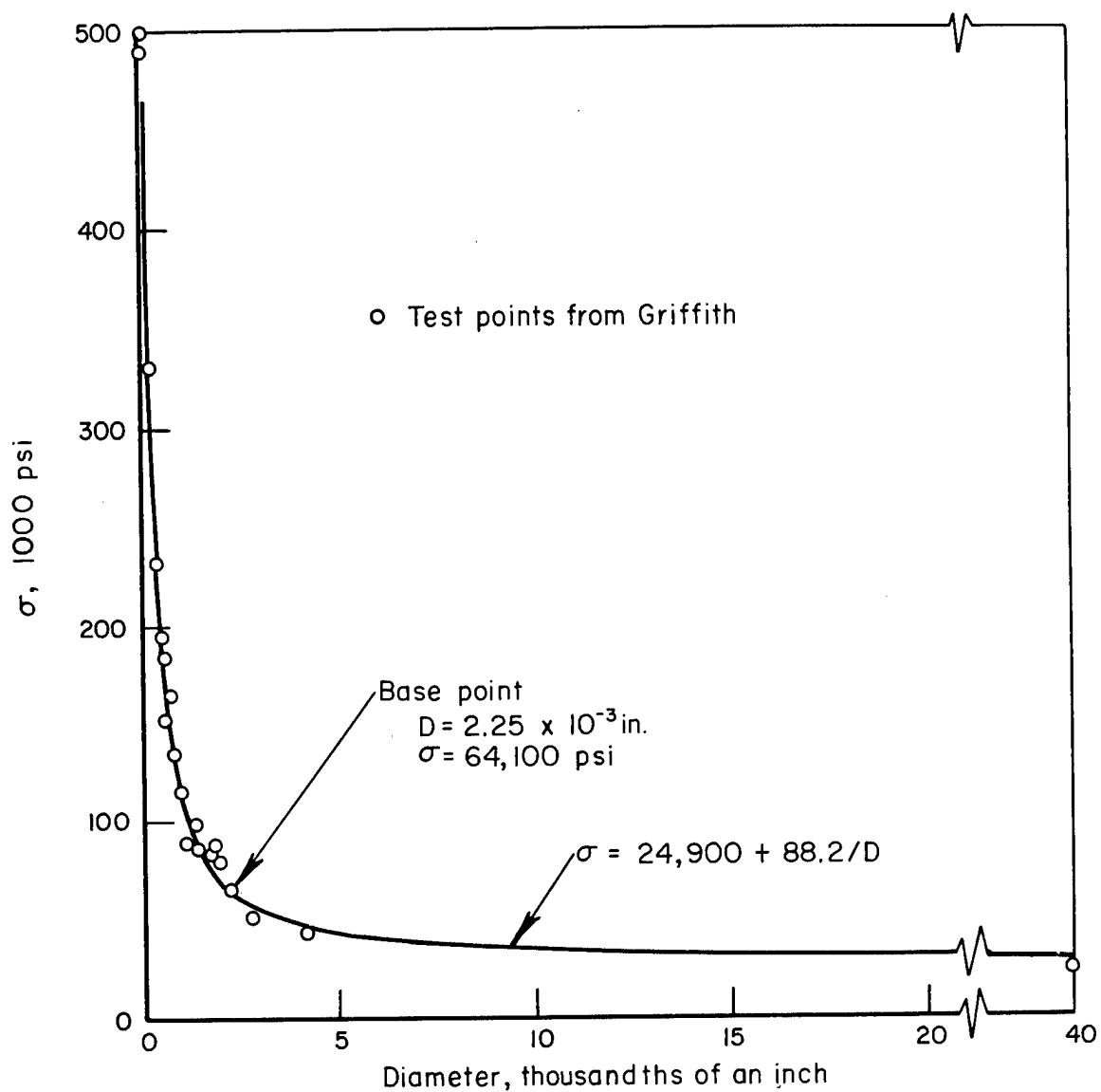
FIGURE 20. COMPARISON BETWEEN SKIN THEORY AND TEST DATA FOR GLASS FIBERS

From Reference (A-7).

It can be shown that, as the diameter increases, the proportion of load carried by the skin decreases and, consequently, the apparent strength of the body will decrease. The nature of the predicted decrease is qualitatively similar to that predicted by the Weibull theory. An example is given in Figure 20, in which Shanley[A-7] used this approach to describe Griffith's data on fracture strength of glass fibers. It can be seen that the data are satisfactorily described by this method.

This approach can also predict the observed effects of stress distribution on apparent fracture strength. Again, consider the relative behavior of specimens subjected to tension and bending. In bending, this contribution is the load multiplied by the distance of the neutral axis. Thus, the relative contribution of the skin (for a given specimen size) will be greater in bending than in tension and the apparent strength in bending will be higher than that in tension, corresponding to observed behavior. The size effect is also predicted in bending as shown in Figure 21. This curve shows the correspondence of predictions of the skin theory with data obtained on various sizes of plaster bend specimens.
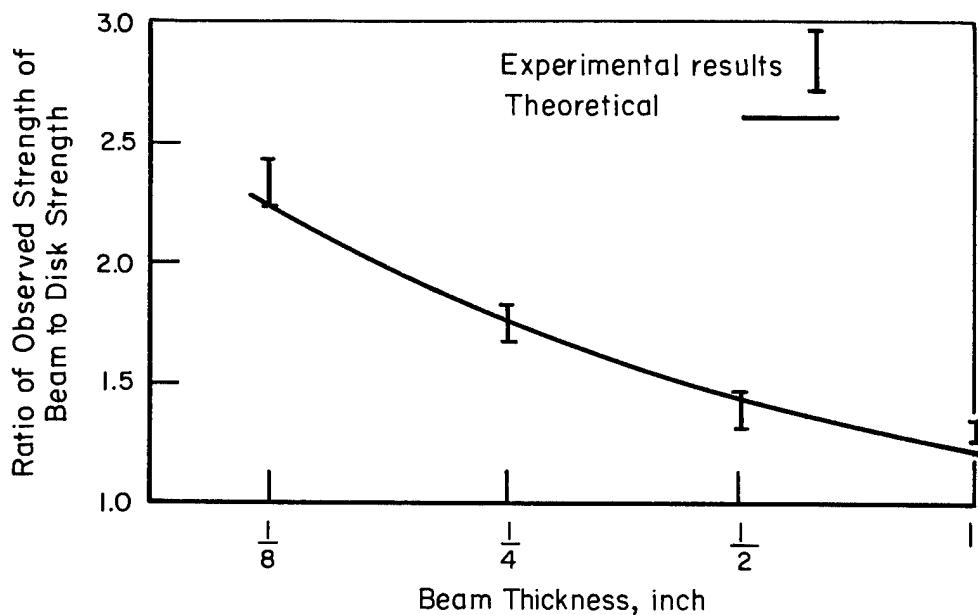

FIGURE 21. COMPARISON BETWEEN SKIN THEORY AND BEND-TEST DATA FOR PLASTER BEAMS

Ratio of Young's moduli = 2.36
Ratio of strength = 2.46
Thickness of skin = 0.03 inch
From Reference A-8.

The skin approach does not predict an effect of length on fracture strength. Since length effects are observed, it is likely that this theory, if basically applicable, would have to be supplemented by some weakest-link-type approach, which would account for the fact that the fracture will occur at the weakest cross section.

It should also be noted that Weibull's treatment included consideration of the possibility that the strength might be limited by surface effects. His considerations were limited to surface flaws. As with other approaches, this has never been adequately studied.

Recapitulation

There are various theories available for describing the strength characteristics of brittle materials. No one theory has been shown to be definitively superior to the others. Nor has any one theory as yet been shown to be consistently adequate in its ability to describe the phenomena. The most popular theory and, indeed, the most appealing is presently that of Weibull. Although several studies have been aimed at verifying this theory, most have ended up evaluating their data on how well it fits the Weibull predictions.

The greatest success of the Weibull theory has been in predicting the variation of mean strength with specimen size and stress distribution. Let us consider some of the limitations of the Weibull theory.

An important requirement of a statistical formulation for brittle-fracture strengths is the ability to predict, from a relatively small sampling, stresses associated with a low probability of fracture, i.e., the low-fracture probability end of the distribution curve. By definition, the low-probability end of a distribution curve cannot be described by a small sampling, although a reasonable estimate of the mean strength can be obtained. Where sufficient data have been obtained, it has been found that the Weibull parameters describing the data in the vicinity of the mean strength did not pertain to the low strength end of the curve.[A-9,A-10] An example is shown in Figure 22, where bend strength data are plotted on Weibull coordinates. A linear plot on these coordinates indicates the adequacy of the Weibull function in describing the data. The parameters of the distribution are determined from the slope and intercept of the line. It is seen that two lines are required to fit the data. Weibull refers to this as "complex" behavior. It is apparent that parameters obtained on the basis of the data near the mean strength are inadequate for describing the behavior in the low-fracture-probability part of the curve. But, this is precisely the part of the curve which is of greatest interest to the designer!

Along the same line, much interest has been expressed in the zero strength (the nominal stress below which there is a zero probability of fracture). According to the Weibull treatment, this value should be a constant independent of size and stress distribution. Several mathematical and graphical techniques have been devised to determine this value. These techniques applied to available data indicate that this value is not a constant but may depend on specimen size and stress distribution. More disturbing is the fact that experimental values of strengths lower than the calculated zero strength have been observed.[A-9,A-10]

In brief, our understanding of brittle fracture is not adequate to justify extensive reliance on any mathematical treatment at this time.
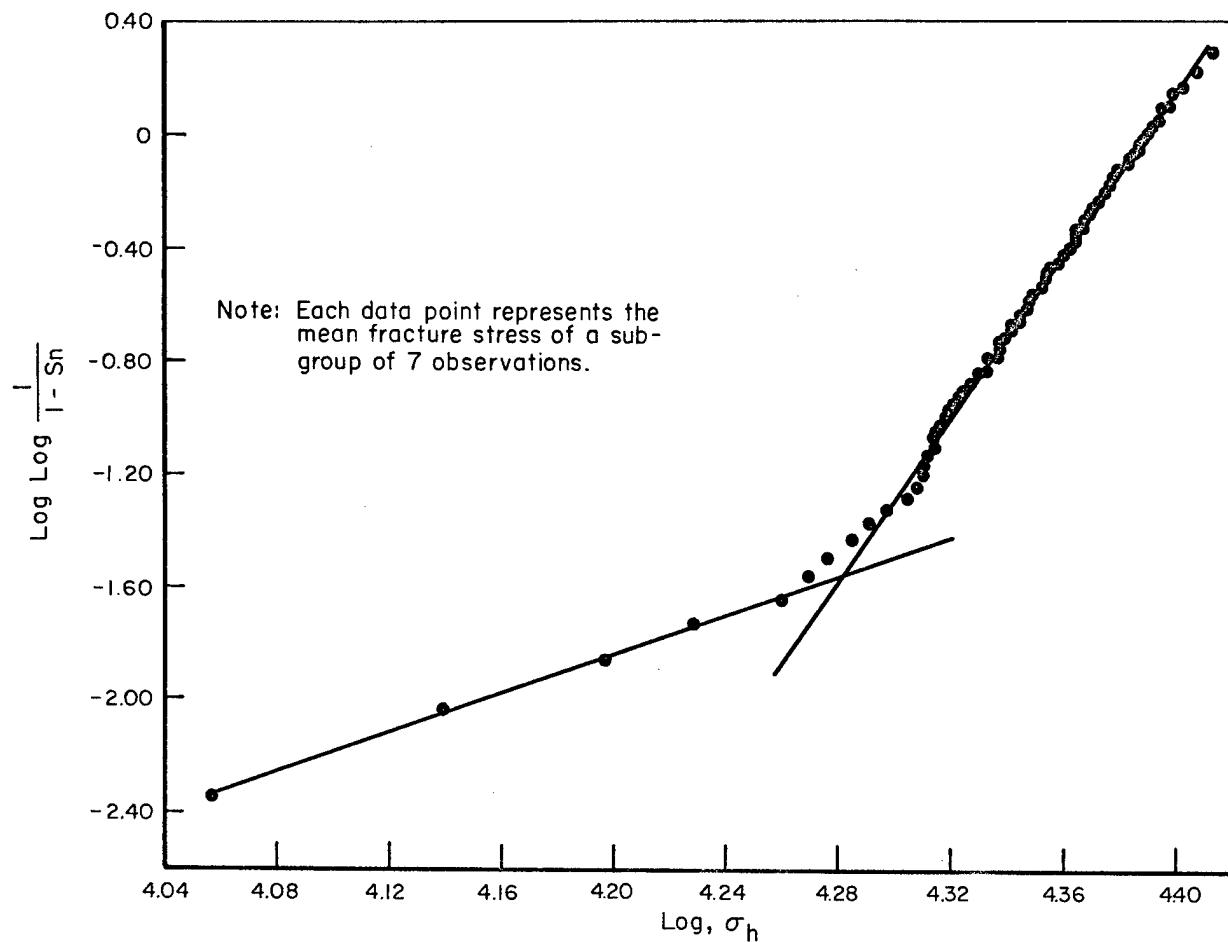
FIGURE 22. STRENGTH DISTRIBUTION OF REFRACTORY PORCELAIN
RODS PLOTTED IN WEIBULL COORDINATES

From Reference (A-9).

Guidelines to Design

As was indicated previously, technology demands that we take advantage of the unique properties of brittle ceramics. We cannot wait until adequate theories are developed. Indeed, brittle materials are currently being employed as stressed components. Until rational design philosophies are developed, design with these materials must be highly conservative and based largely on experience. Proof tests should be employed wherever possible. Also, the geometric design should avoid small-radius re-entrant corners and other stress concentrations. Components should be closely inspected to detect macroscopic flaws. Special care should be exercised in assembly to avoid unintentional prestressing and surface damage.

Other considerations should be incorporated depending on the specific design.[A-2] As an example, studies of the use of graphite for the leading edge of a re-entry vehicle led Anthony and co-workers[A-11] to a set of design principles. These principles were summarized in a recent paper[A-12] as follows:

(a) Attachments between leading-edge elements and the supporting wing or surface structure must be completely nonredundant so that unknown loads are not introduced by relative deformation under the applied airloads and temperature gradients, and also so that misfits during assembly will not introduce unknown initial stresses into the nonmetallic elements. This nonredundancy must exist not only in all three translational directions but also rotationally about the three axes.

(b) Where the nonmetallic structural elements are attached to the metallic structures, thermal-expansion differences at the mating surfaces must be accommodated in order to avoid excessive induced stresses or excessive lack of fit due to differential thermal expansion. The requirements for achieving this condition with any type of attachment design have been developed and are explained in Reference (A-11).

(c) Integral parts should be used so far as possible to minimize mechanical joints. Joints have the basic problem of achieving uniform bearing pressures in a nonyielding material. A mechanical fastener in a hole, for instance, requires extremely close tolerances and very smooth surface finish to avoid all of the load being taken on a few high contact points, with resulting large bearing stress concentrations.

In more recent work, Anthony and Dukes[A-13] have reinterpreted the use of a safety factor in these applications to include consideration of the lower probability of occurrence of extreme loadings to effect a tradeoff between weight and reliability. The use of such approaches as these can result in the successful application of ceramics as structural components. As the understanding of brittle-fracture phenomena improves, we will be able to take increasing advantage of these materials and approach "optimum" design.

References for Appendix

(A-1) Rudnick, A., Carlson, R. L., and Manning, G. K., "Investigation of Feasibility of Utilizing Available Heat-Resistant Materials for Hypersonic Leading Edge Applications. VI. Determination and Design Application of Mechanical Properties of Bare and Coated Graphite", WADC TR 59-744 (July 1960).

(A-2) Barnett, R. L., "Review of Structural Design Techniques for Brittle Components Under Static Loads", ARF Report No. 8259, Phase 1 - Task 2, prepared under Contract AF 33(657)-8339 (May 1963).

(A-3) Thomas, W. F., "An Investigation of the Factors Likely to Affect the Strength and Properties of Glass Fibers", Physics and Chemistry of Glasses, VI (N1), 4-18 (February 1960).

(A-4) Epstein, B., "Statistical Aspects of Fracture Problems", J. Appl. Physics, 19, 140-147 (February 1948).

(A-5) Weibull, W., "A Statistical Theory of the Strength of Materials", Ing. Vetenskaps Akad., 151 (1939).

(A-6) Daniels, H. E., "The Statistical Theory of the Strength of Bundles of Threads", Part I, Proc. Roy. Soc., London, 183, 405-435 (1945).

(A-7) Shanley, F. R., "On the Strength of Fine Wires", Research Memorandum, USAF Project RAND, AD 144288 (September 26, 1957).

(A-8) Barenbaum, R., and Brodie, I., "Measurement of the Tensile Strength of Brittle Materials", Brit. J. Appl. Phys., 10, 281 (June 1959).

(A-9) Salmassy, O. K., Bodine, E. G., Duckworth, W. H., and Manning, G. K., "Behavior of Brittle State Materials", WADC TR 53-50, Part II (June 1955).

(A-10) Bortz, S. A., and Weil, N. A., "Effect of Structural Size; The 'Zero Strength'", ASD TR 61-628, Part II, 10-74 (April 1963).

(A-11) Anthony, F. M., et al., "Investigation of Feasibility of Utilizing Available Heat-Resistant Materials for Hypersonic Leading Edge Applications", WADC TR 59-744 (November 1960).

(A-12) Dukes, W. H., and Anthony, F. M., "The Design of Structural Elements With Brittle Materials", presented at the ASM Golden Gate Conference, (February 13, 1964).

(A-13) Anthony, F. M., and Dukes, W. H., "Evaluation of ZrB_2-MoSi_2 as a Structural Refractory Ceramic Body", Bell Aerosystems Company Report No. 2178-900203, prepared under Contract No. AF 33(657)-11284 (March 1964).